Journal of Engineering and Technology

of the Open University of Sri Lanka

Volume 07 No. 02 September 2019 ISSN 2279-2627

All correspondences should be addressed to:

Editor in Chief – Journal of Engineering and Technology
Faculty of Engineering Technology
The Open University of Sri Lanka
Nawala, Nugegoda
Sri Lanka
Email: bcliy@ou.ac.lk, Telephone: +94112881111

The Journal of Engineering and Technology of the Open University of Sri Lanka is a peer-reviewed journal published bi-annually by the Faculty of Engineering Technology of the Open University of Sri Lanka. The journal accepts original research articles based on theoretical and applied research in the area of Engineering and Technology in all specializations.

Published in December 2019

Contents

Volume 07 No. 02 September 2019 ISSN 2279-2627

Study of Variable Amplitude in Cyclic Loading

Nimali T. Medagedara

Dept. Mechanical Engineering, The Open University of Sri Lanka, Nawala, Nugegoda, Sri Lanka

Corresponding Author: tmmed@ou.ac.lk, Tele: +94112881113

Abstract – *Fatigue failure often initiates from a point of stress concentration, where the local deformation is inelastic. Fatigue is produced by the repeated application of cyclic loads and prediction of fatigue failure is important at the design stage of components to minimize the risk of failure. Therefore, the analysis of elastic-plastic deformation and predict the behavior of the component is an essential for fatigue durability assessment of engineering components. Due to the lack of valid analytical methods to perform an accurate stress analyses, many engineers rely on finite element methods to evaluate elastic-plastic stress/strains in complex components. Many commercially available finite element software use simple flow rules and commonly known yield criteria for the stress/strain calculations. In this study, the finite element method was used to analyze a notched specimen made of mild steel which was subjected to cyclic tensile and torsional loading. The results obtained for strain were compared using a Neuber method.*

The comparison concludes that strain values resulted from Neuber method are 36% higher than the that from Finite Analysis method. This infers that Neuber evaluation method over estimates the results from FEA method (1). However, for an exact validation of the FEA model under realistic conditions further experimental analysis is needed.

Keywords*: Cyclic Loading, Finite Element Analysis, Neuber Equation*

1 INTRODUCTION

Finite Element Analysis (FEA) is a computer-based numerical technique for calculating the strength and behaviour of engineering structures. It can be used to calculate deflection, stress, vibration, buckling behaviour and many other phenomena. It can be used to analyze either small or large-scale deflection under loading or applied displacement. Finite element method can be used to analyze both elastic deformation and plastic deformation.

Mild steel is used in a wide range of industrial applications that involve cyclic loading. It is used mainly used for bridges and for manufactureing bolts and fasteners as it has required strength and ductility. These applications may involve multiaxial loading, which can be more damaging for the mateial than the uniaxial condition, especially for nonproportional loading. Hence, an understanding of the cyclic stress-strain response and of the fatigue behaviour under multiaxial loading of these materials is important for safer engineering design.

Finite Element Analysis enables detail evaluation of complex structures in a computer, at the designing stage of these structures. This study investigated the deformations of mild steel having Elastic modulus of 2.08E05 MPa, Poisson ratio, 0.3 and modulus of rigidity, 80 GPa under cyclic loading. The specimen modelling and finite element analysis were carried out by using ABAQUS Code. The new cycle counting method, the Stress Scale Factor (SSF) virtual cycle counting, is based on the SSF equivalent shear stress early proposed by the Benham et al (1996).

2 SAMPLE DESIGN AND FINITE ELEMENT ANALYSIS

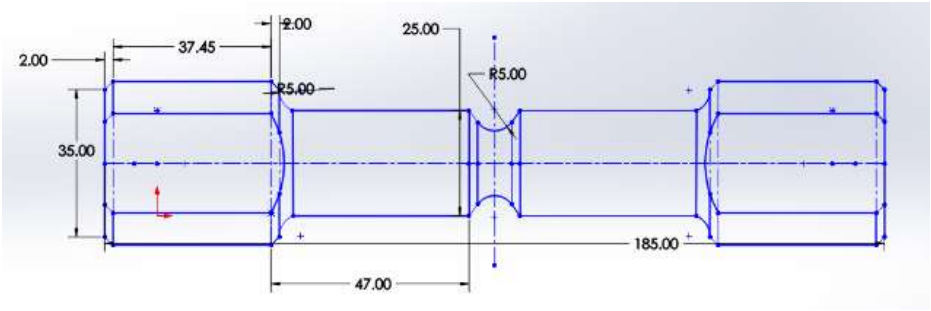

Fig. 1: Dimensions of the specimen

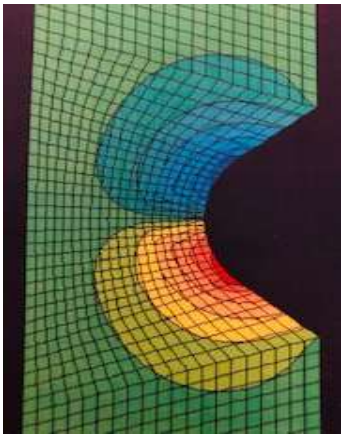

Fig. 2 3D view and the finite element model
(a) 3D view of the specimen (b) Abacus model

Fig. 1 shows the dimensions of the notched specimen and figure 2a and 2b, the 3D view and the finite element model of the specimen. The specimen was modelled by using ABAQUS software and the total number of elements used for the model was 2600. For the critical analysis 600 elements were used to define the mesh in notch area as the notch area is the main concern of the investigation and this number of elements satisfy the computer programme constrains.

3.0 ELASTIC STRESS/STRAIN ANALYSIS OF THE SPECIMEN

3.1 Tensile Loading

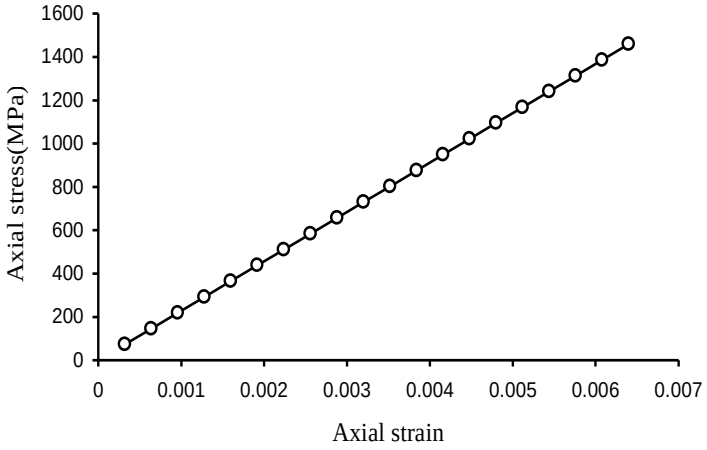

Fig. 3: Linear variation between axial stress / strain (S22-E22) at the notch root

A relationship between the stress and the strain at the notch root was found by applying a 0.2 mm axial displacement to the specimen. As shown in Fig. 3, it behaved linearly as expected in the elastic region. The gradient of the graph was calculated to be 208,000 MPa and it is close to the established values of modulus of elasticity.

In practice, fatigue failure usually occurs at notches or stress concentrations. Stress concentrations often result maximum local stresses, σ_{max}, at the discontinuities, which are many times greater than the nominal stress (S) of the member. In ideal elastic members, the ratio of these stresses is designated as K_t, the theoretical stress concentration factor Knop etal , 2000). However, there are a number of assumptions in the local strain approach that could contribute to the difference between low and high K_t specimens. One of these assumptions is that Neuber's rule can adequately estimate the stress and strain at the root of the notch (Peterson, 1974).

Fig. 4 shows the FEA results of (S22 direction) stress distribution throughout the specimen when a 0.2 mm axial displacement is applied under the elastic condition. Maximum stress can be observed at the notch root.

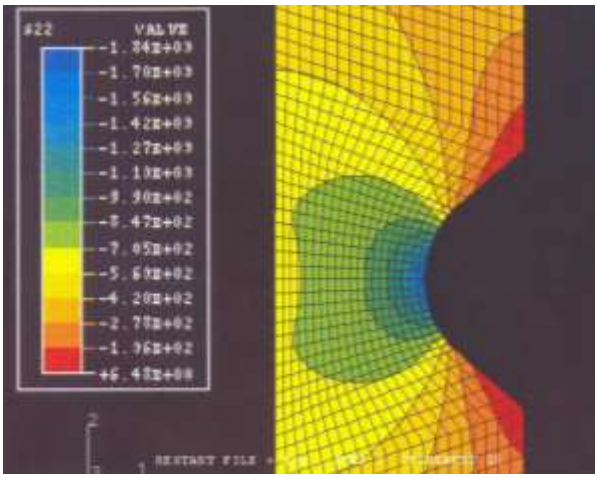

Fig. 4: The elastic stress distribution near the notch root

Several parts of the stress distribution in the vicinity of the notch root can be seen. The first zone includes the maximum stress. Behind the third zone, the stress values are comparatively small.

4.0 THEORETICAL STRESS CONCENTRATION FACTOR ANALYSIS:

An estimate to the magnitude of the stress concentration factor may often be obtained by undertaking a manual analysis. Considering the Figure 4, from the FEA elastic results, for an applied displacement of 0.2 mm, the theoretical stress concentration factor K_t was calculated and the value was 1.8, whereas the established K_t value from handbook (Knop et al , 2000) is 1.6 resulting 12.5% higher value.

5.0 ELASTIC/ PLASTIC STRESS ANALYSES:

Plasticity deals with the methods of calculating stresses and strains in an irreversibly deformed body after all elements of the body have yielded. It is necessary to establish equations of equilibrium and compatibility, and to determine the experimental relations between stress and increments of strain. The most difficult problem to solve in plasticity is those of constrained plastic flow (Buczynski, and Glinka, 1997). Total strain within elastic-plastic range can be derived as:

$$\varepsilon = \frac{\sigma}{E} + \left[\frac{\sigma}{K}\right]^{1/n}$$

Where 'E' is the modulus of elasticity, 'σ' is the direct stress, 'K' is strength coefficient and 'n' is strain-hardening exponent (Benham, et al 1996).

For the plastic analysis the model was subjected to isotropic hardening behavior and for the analysis yield stress of the material and the plastic strain limits were given as input to the software programme.

Plastic strain is the portion, which cannot be recovered on unloading. Plastic strain produces both changes in grain shape and, on a very much smaller scale, changes in the distribution of lattice defects or dislocations (Medagedara and Sarathchandra 1994). It is these changes that cause strain hardening. Plastic strain can produce changes in the yield point of single crystal of pure metal (Shang et al , 1999).

6.0 TENSILE LOADING

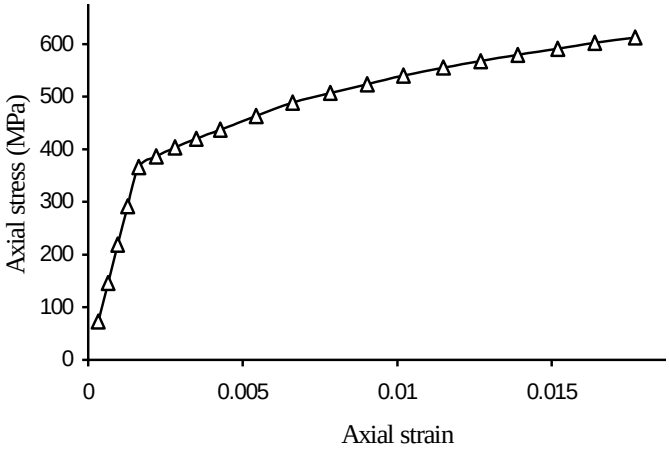

Fig. 5: The stress–strain response at the notch root for tension (0.2 mm displacement) in elastic-plastic condition

As in the Fig. 5, when applying an elastic-plastic load, the graph behaves linearly up to the stress of 350 MPa and then it changes to plastic behavior. Considering the linear portion, gradient of the graph was calculated to be 208,000 MPa, which is close to the modulus of elasticity of the material.

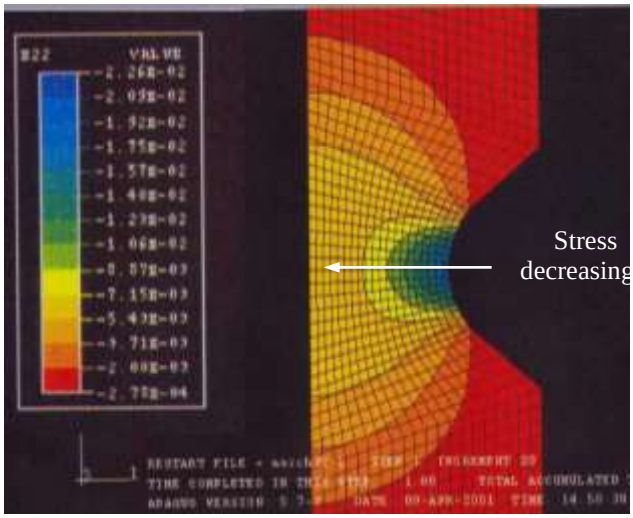

Fig. 6: Area of the plastic strain when applying 0.2 mm axial displacement

The elastic-plastic stress/strain distribution near the notch root exhibits first a peak point and then a decreasing dependence to the distance from the notch root. Few different stress/strain distributions in the vicinity of the notch root can be particularly distinguished as in Fig. 6.

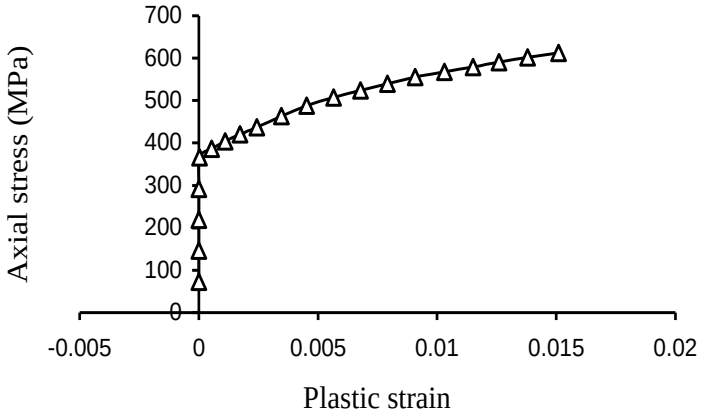

Fig. 7: Relationship between axial stresses against plastic strain (0.2mm axial displacement)

Fig. 7, shows the plastic strain, which cannot recover on unloading. Plastic strain starts from 350 MPa of axial stress and showing its continuous increase with the strain amplitude.

7.0 NEUBER ANALYSIS

7.1 Estimation of elastic-plastic stress concentration factor:

Elastic-Plastic stress concentration factor was estimated using FEA results and using Neuber equation $Kt^2Se = \sigma\epsilon$. Considering the Fig. 6, from the FEA results, for an applied displacement of 0.2 mm, the theoretical stress concentration factor K_t was calculated and the value was found as 1.6. This value is compatible with the theoretical K_t value given in stress concentration graph (Knop et al , 2000).

8.0 MODELLING CYCLIC STRESS-STRAIN HYSTERESIS BEHAVIOUR

Cyclic stress-strain curves are useful for assessing the durability of structures and components subjected to repeated loading. The response of a material subjected to cyclic inelastic loading is in the form of a hysteresis loop. The area within the loop is the energy per unit volume dissipated during a cycle. It presents a measure of the plastic deformation work done on the material.

8.1 Cyclic Axial load

For elastic plastic condition, a cyclic axial load was applied to the ABACUS model with a cyclic load (with reversible axial displacement) applied as axial displacement varying with time is shown in Fig. 8.

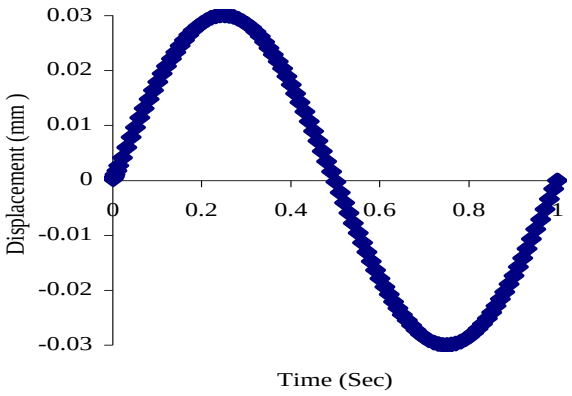

Fig. 8: Applied axial displacement against time for cyclic loading

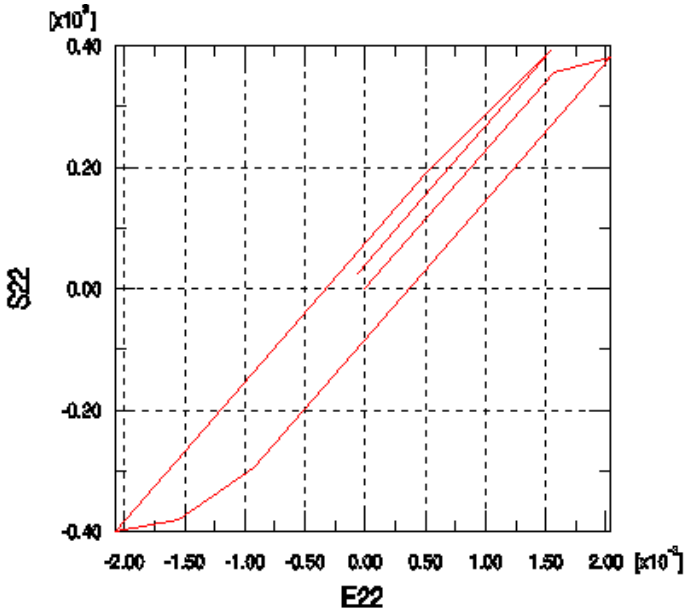

Fig. 9: Axial stress-strain (S22-E22) variation at the notch root (FEA results) for ±0.03 displacements (cyclic loading)

The Fig. 9 shows the hysteresis loop obtained from cyclic axial loading. The loop has a little plastic energy and the maximum strain range of the loop is 0.002. Using material cyclic stress-strain curve and Neuber curve, hysteresis loop was predicted for same cyclic axial load. Initially the hysteresis loop was developed for the material by using the equation, and developed the other curves by using Neuber equation $Kt^2Se = \sigma\epsilon$. For stress concentration factor K_t, a value of 1.6 was used and developed several curves by changing nominal stress value (S). Then common values were found from the both graphs to predict the Neuber hysteresis loop as shown in Fig. 10.

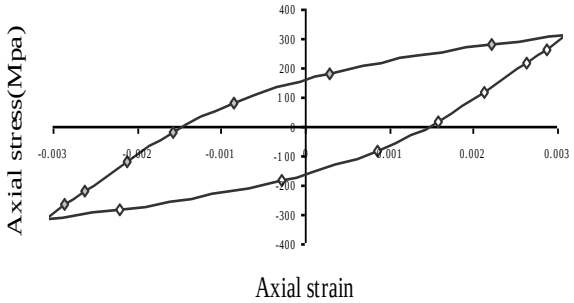

Fig. 10: Predicted hysteresis loop from Neuber equation for same FE load

Comparing the strain values obtained from the finite element analysis and the value achieved from the predicted hysteresis loop for cyclic loading condition, the strain predicted from Neuber was 36% than that obtained from finite element analysis.

9.0 CONCLUSIONS

An approximate model for elastic–plastic stress–strain analysis of a notched bar under variable amplitude tension and torsion cyclic loading is presented. A detailed FE analysis was performed for an axisymmetric steel bar of circular cross-section with a circumferential notch subjected to different elastic, elastic-plastic loading cases. The comparison of the finite element results with that of Neuber analysis shows that the latter results were over estimated than that of the FEA. ABAQUS software can provide sufficiently accurate estimations for elastic–plastic notch stresses and strains for elastic, elastic-plastic cyclic loading conditions. Neverthless, further research is required to consolidate the validity of results obtaned from finite element method.

REFERENCES

Benham P.P., Crowford R.J. and Armstrong C.G., 1996, Mechanics of Engineering Materials, 2nd Edition, Longman Group, pp 463-544

Knop M., Jones R., Molent L. and Wang C., 2000, On the Glinka and Neuber Methods for Calculating Notch Tip Strains Under Cyclic Load spectra, Int. J fatigue Vol. 22, pp 743-755 Elsevier Science Ltd.

Peterson R.E, 1974, Stress Concentration factors, New York: Wiley

Buczynski, A., and Glinka, G., 1997, Elastic-Plastic Stress-Strain Analysis of notches under non-proportional loading, Proceeding of the 5th international conference on Biaxial/Multiaxial Fatigue and Fracture Cracow'97, Poland, pp 461-479.

Shang, D., Wang D., and Yao W. X., 1999, A simple Approach to the Description of Multiaxial Cyclic stress-strain relationship, Int. J fatigue, Vol. 22, pp 251-256.

Medagedara N.T, Sarathchandra P.D.,1994. Elastic-Plastic Stress/Strain Behaviour of Notched shaft under axial and torsional cyclic loading and proportional loading (comparison of experimental and finite element results, International Symposium of research Students on Material Science and Engineering (ISRS – 2004),Madras, India.

An Algorithm for the Holzer Method & Holzer Correction Formula for Torsional Vibration Analysis

D.T.D.M. Dahanayaka[1*], A.R. Lokuge[1], Iresha U. Atthanayake[1]

[1] Department of Mechanical Engineering, The Open University of Sri Lanka, Nawala, Nugeogda, Sri Lanka.

*Corresponding Author: email: tharudahanayaka@gmail.com , Tele: +9477 0610713

Abstract –. *This paper investigates the development of an algorithm for the Holzer method and Holzer correction formula. Natural Frequency & Mode shapes are considered as dominant factors in a multi degrees of freedom system design. The Holzer method is used to calculate Natural Frequency mostly in torsional vibration systems, which is a tabular method for the analysis of multi mass lumped-parameter systems. It is considered as a trial and error method due to the time-consuming steps of calculation. When the number of rotors exceed than three it becomes extremely difficult to determine Natural Frequency in calculations by hand. In order to address these problems, an algorithm is developed to calculate Natural Frequencies. A user-friendly software interface is also integrated to enter parameters and variables of the torsional system. Using these data, the proposed algorithm is able to determine and displays whether the user given frequency is the natural one or not. If it is not the Natural Frequency, most accurate Natural Frequency can be obtained by the algorithm it-self. Further proposed software facilitates to calculate Natural Frequency in a given range in a user-friendly interface. By changing the parameters, it is able to obtain the relevant Natural Frequency which is necessary when optimizing a design. As well as the program produces the behavior of the system with change in parameters through graphs.*

Keywords*: Holzer Correction Formula, Holzer Method, Natural Frequency, Torsional Vibration System, Vibration*

Nomenclature

i - number of rotors
T - Torque (Nm)
n - Final rotor
G - Modules of rigidity (Nm^{-2})
L - Length of the shaft (m)
J - Polar moment of inertia of the shaft cross section (m^4)
d - diameters for different shaft lengths (m)

Greek Letters

ω - frequency ($rad\ s^{-1}$)
θ - Angular position of the disk (rad)

Subscripts

I_i - moment of inertia of i^{th} rotor (kgm^2)
a_i - Angular Strains (rad)
K_i - torsional stiffness of i^{th} shaft ($Nmrad^{-1}$)
ω_n - Natural Frequency ($rads^{-1}$)

1 INTRODUCTION

Vibration affects the performance of systems favorably as well as unfavorably. Unfavorable vibrations are detrimental for systems, and designers often try to avoid them within their approaches for the design. The most harmful situation is that the acting frequency falls within the range of Natural Frequency. Therefore, the Natural Frequency of the system should be found first. The most common and traditional method is to build a physical model and follow the "trial and error" method. This is time consuming and the accuracy of those calculations depends on the performance of the person doing it. Second method is the modern approach to build an analytical model to represent the system and predict the consequences very early before the manufacturing process starts. In an analytical model, equations for each degree of freedom (DOF) are needed. This is not practical with systems which have more than three DOFs. To overcome this issue the Holzer Method is introduced to the design world. Instead of going through many calculations Holzer method allows us to determine Natural Frequency by filling a table of elements. Natural Frequency is the frequency at which a system tends to oscillate in the absence of any driving force. When a system vibrates at a frequency equivalents to its Natural Frequency, its vibration amplitude increases significantly which could lead to irreversible damage. Sometimes we may find different configurations of vibrations such as linear vibration, rotational vibrations and torsional vibration.

Torsional vibration is an oscillatory angular motion that can happens in mechanical systems when there is a non-uniformity of the torque developed or transmitted. It occurs in the shafting systems. Torsional vibration is gaining the attention of the industrial community because of its high influence in the machine components. Under some environments, rotational elements can fail due to torsional vibration. Torsional vibration is a complex vibration having different structures, with different parameters, the free vibration and forced vibration systems. This vibration cannot be detected easily. Even though it's amplitude can be detected using special measuring equipment. Natural frequency is a main factor in a torsional system in order to control the torsional vibration. It is easy to calculate the Natural Frequency, if a torsional system consists of two or three rotors. When the number of rotors increase, it becomes extremely difficult to determine the Natural Frequency. Hence the Holzer method and Holzer correction formula is used. Natural Frequencies and mode shapes are determined by assuming a frequency and starting with a unit amplitude at one end. But, if the manual calculation is done, the major challenges of this method are high time consumption and even a small error affects the result.

In order to address these problems, in this study a software was developed. The user only needs to provide parameters of the torsional system. Using these data, the software program determines and displays whether the frequency which is given by the user is natural or not. If it is not a Natural Frequency, most accurate Natural Frequency can be obtained via the program. Further proposed algorithm facilitates to calculate Natural Frequency in a given range easily. Also, it provides all the frequencies and necessary values through a graph and tables for given range are provided. By changing the parameters, it is able to obtain the relevant Natural Frequency which is necessary to operate the torsional system. As well as the program produce a graphical behavior of the parameters. Hence the proposed algorithm can be identified as user-friendly software. J Quiroga *et. al.* (2019) has developed a system to check only the effectiveness of Holzer Method using ANSYS. According to the literature review this proposed algorithm is a novel method to find natural fre20quencies of complex torsional systems.

2 METHODOLOGY

The proposed algorithm is programmed in visual studio 2012 platform. Holzer method was used to develop the algorithm. Then mathematical calculations and relations were developed between parameters using visual basic codes.

A. Analytical models used for various situation

In the algorithm we considered two torsional vibration cases i.e. straight line free torsional vibration system and forced torsional vibration system of which typical schematic diagrams are shown in figure 1 and figure 2 respectively.

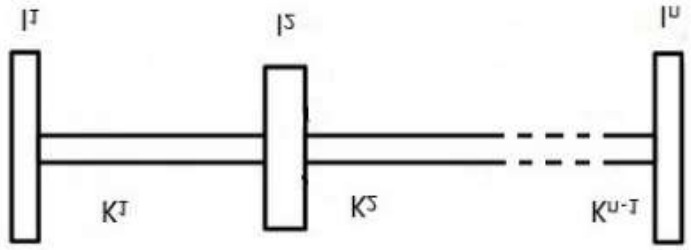

Fig. 1. Straight line free torsional vibration system

Table 1 Holzer table for free vibration

1	2	3	4	5	6	7	8
i	I_i	ω^2	a_i	$I_i\omega^2 a_i$	$[\sum I_i\omega^2 a_i] = Y_i$	Ki	$[(\sum I_i\omega^2 a_i / Ki)] = X_i$

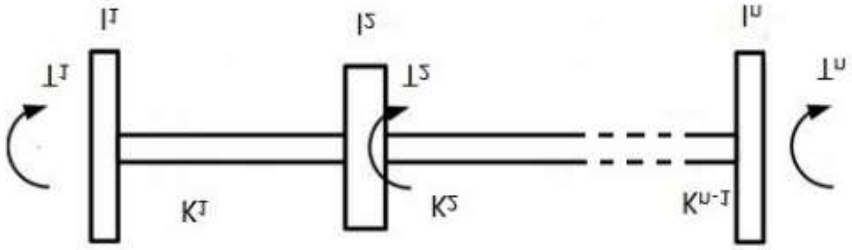

Fig. 2. Straight line forced torsional vibration system

Table 2 Holzer table for forced vibration

1	2	3	4	5	6	7	8	9
i	I_i	ω^2	a_i	$I_i\omega^2 a_i$	T	$[\sum (I_i\omega^2 a_i + T)] = Y_i$	Ki	$[\sum (I_i\omega^2 a_i + T)/ Ki] = X_i$

The Holzer table prepared for two cases are shown in Table 1 and Table 2.

Angular Strains were calculated according to the Holzer method,

$$\begin{aligned} a_1 &= 1 \\ a_2 &= a_1 - X_1 \\ a_3 &= a_2 - X_2 \\ . & \quad . \\ a_n &= a_{n-1} - X_{n-1} \end{aligned}$$

Via this software Natural Frequency can be obtained easily for straight line free and forced vibration torsional systems. If the frequency value which user entered is not the Natural Frequency, then a frequency which close to the Natural Frequency is provided to the user using Holzer Correction Formula. Then assume,

$$I_n = I^*$$

And I^* value was determined, assuming,

$$Y_n = 0, \text{ Then, } \delta I_n = I_n - I^*$$

using the correction formula,

$$\delta\omega^2 = \{[-\omega^2 (\delta I_n) a_n^2] / [\sum_{r=1}^{n} I_r a_r^2]\}$$

then corrected Natural Frequency ω_n, was obtained

$$\omega_n^2 = \omega^2 + \delta\omega^2$$

Figure 3 shows a typical schematic diagram for a straight line one end fixed torsional vibration system.

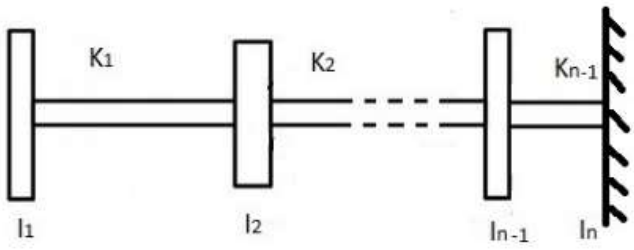

Fig. 3. Straight line one end fixed torsional vibration system

This system has only one end fixed and it is considered as a rotor having a very large moment of inertia. That is I_n has infinite inertia ($I_n \approx \infty$). In this system Natural Frequency can be obtained considering a_n. If the user entered a frequency value not equal to Natural Frequency, then a frequency which is closer to Natural Frequency is provided to the user using Holzer Correction Formula. Then assume,

$$K_{n-1} = K^*$$

And K^* value was determined, assuming, $a_n = 0$

Then,

$$\delta K_n = K_{n-1} - K^*$$

using the correction formula,

$$\delta\omega^2 = \{[(\delta K_n)\, a_n^2] / [\,{}_{r=1}\textstyle\sum^{n-1} I_r\, a_r^2]\}$$

then corrected Natural Frequency ω_n, was obtained

$$\omega_n^2 = \omega^2 + \delta\omega^2$$

For example, to calculate the Natural Frequency for the given below rotor system as shown in Fig.4, Let us assume that the Natural Frequency of vibration is ω = 1.05 rad s^{-1}. That is ω^2=1.1 rad s^{-1}. I_1 =1 kgm^2, I_2=2 kgm^2, I_1 =2 kgm^2, a_1=1 and K_1=1, K_2=2. If do the calculations manually, these steps need to be done.

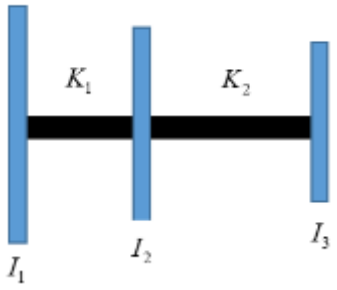

Fig. 4. Straight line free torsional vibration system

1. $I_1\omega^2$ = 1.1
$I_1\omega^2 a_1$ = 1.1
$\Sigma I_1\omega^2 a_1$ = 1.1
$\frac{1}{K}\Sigma I_1\omega^2 a_1$ = 1.1

2. $I_2\omega^2$ = 2.2
$a_2 = a_1 - [\frac{1}{K}\Sigma I_1\omega^2 a_1]$
= -0.1
$I_2\omega^2 a_2$ = -0.22
$\Sigma I_2\omega^2 a_2$ = 0.88
$\frac{1}{K}\Sigma I_2\omega^2 a_2$ =0.44

3. $I_3\omega^2$ = 2.2
$a_3 = a_2 - [\frac{1}{K}\Sigma I_2\omega^2 a_2]$
= -0.54
$I_3\omega^2 a_3$ = -0.19
$\Sigma I_3\omega^2 a_3$ = -0.31

Table 3 Holzer table for given example

i	I_i (kgm^2)	$I_i\omega^2$	a_i	$I_i\omega^2 a_i$	$\Sigma I_i\omega^2 a_i$	K_i	$\frac{1}{K}\Sigma I_i\omega^2 a_i$
1	1	1.1	1.0	1.1	1.1	1	1.1
2	2	2.2	-0.1	-0.22	0.88	2	0.44
3	2	2.2	-0.54	-0.19	-0.31		

As shown in Table 3, the sum of values of the column $\Sigma I_i\omega^2 a_i$ is not equal to 0 hence the value of ω = 1.05 rad s^{-1}cannot be the correct Natural Frequency. Therefore, an additional calculation has to be done in order to find the correct Natural Frequency. There are two methods this can be implemented. In analytical method the same calculation process needs

to be done at least twice to get a sufficiently close value to the correct Natural Frequency assuming another frequency value as a Natural Frequency. In the other method which is the Holzer correction formula also requires additional calculation. If do the calculations manually for Holzer correction formula, these steps need to be done. Since the residual torque is not zero, $\omega = 1.05$ rad s^{-1}cannot be the correct frequency

Let us say $I_3 = I^*$ and determine the value of I^*so that $\sum_{i=1}^{3} I_i \omega^2 a_1 = 0$

at the same frequency (ω = 1.05rad s^{-1}) and the same a_r.
then modified row 3 gives,

3	I^*	*1.1 I**	*-0.54*	$0.54I^*$	*0.88-0.594I**		

Therefore,

$$0.88 - 0.594I^* = 0$$
$$I^* = 1.48$$

This means that when $I^* = 1.48$ Kgm^2, the exact Natural Frequency $\omega = 1.05$rad s^{-1}, Now the we can use the correction formula to determine the Natural Frequency of given system

$$\delta I_3 = I_3 - I^* = 2 - 1.48 = 0.52\text{Kgm}^2$$

Using the correction formula

$$\delta\omega^2 = \frac{-\omega^2(\delta I_n)a_n^2}{\sum_{r=1}^{3} I_r a_n^2}$$
$$= \frac{1.1 \times 0.52 \times (0.54)^2}{[1 \times 1 + 2 \times (0.1)^2 + 2 \times (0.54)^2]} = -0.104$$

Corrected frequency ω_n is given by,

$$\omega_n^2 = \omega^2 + \delta\omega^2 = 1.1 - 0.104$$
$$\omega_n = \sqrt{0.996} = \underline{\underline{0.998\,\text{rad s}^{-1}}}$$

Note – In case the value for I^* was obtained as negative, the same process has to be executed for a fresh value for ω_n again.

If the manual calculation was done as above, the major challengers of this method are high time consumption and even a small error affects the result. In order to address these problems, proposed software can be used.

B. Natural Frequency obtain using graphical method
If the user entered two frequency square values (ω_1^2 and ω_2^2) and their residual torque ($[\sum I_i\omega^2 a_i] = Y_i$) Y_1 and Y_2, then Natural Frequency can be obtained using the graphical method as shown in Fig.5

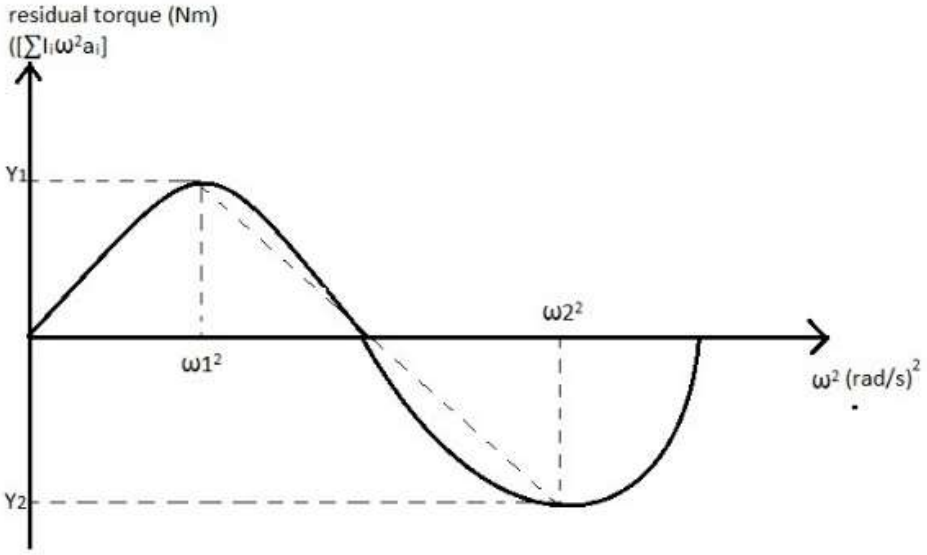

Fig. 5. Natural Frequency using graphical method

C. Calculation of Natural Frequency by changing different parameters

Calculation of Natural Frequency by changing different parameters like I_i and d_{i-1} in a torsional system is the best method to keep the acting frequency away from it and make it easy to select frequency of the motor too. From this proposed software facilitates to change parameters I_i and d_{i-1} for given range and obtain residual torque ($\Sigma I_i\omega^2 a_i$) values in a graph. Through these observations a proposed system can be optimized according to design requirements.

3 SIMULATION EXPERIMENTS AND RESULTS

A. The developed algorithm consists four main options as follows, Natural Frequencies of straight line free torsional vibration system, Natural Frequencies of straight line free torsional vibration with one end fixed system, straight line forced vibration system and Natural Frequencies using graphical method. Parameters need to provide to find the Natural Frequency. Then the proposed algorithm determines and displays Holzer table with the values. Fig.6 shows the way Holzer table values are displayed in the graphical user interface. If it is not the Natural Frequency, most accurate Natural Frequency can be obtained by the program quickly and easily.

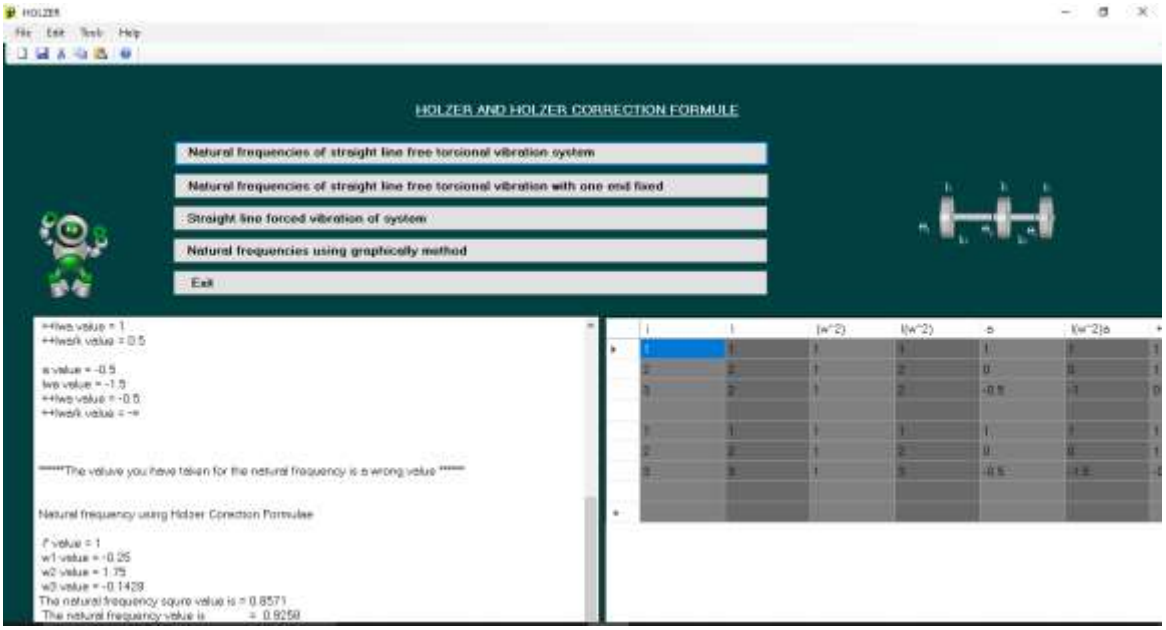

Fig. 6. Holzer table with the values

B. Also proposed software facilitates to calculate Natural Frequency in a desired range. By changing the parameters in the individual components of the system, the necessary graphs and details can be obtained. Because of this option we don't need to make more Holzer tables for each frequency to seek the natural frequency. We can obtain all the necessary accurate details from the graph and tables for a given range. The proposed program determines the Holzer graph and table for each frequency in the given range as shown in Fig.7 and Fig.8.

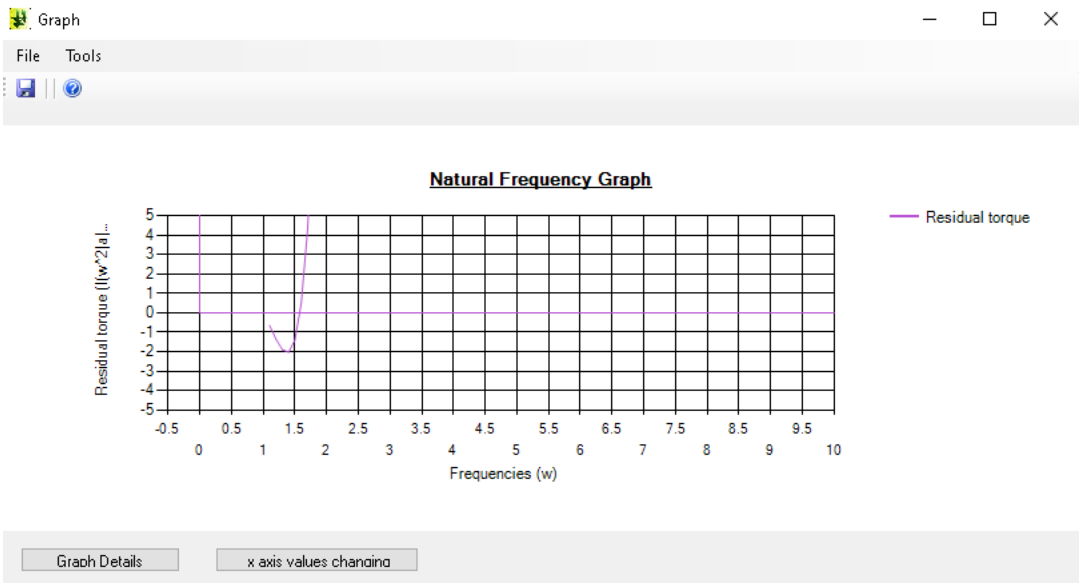

Fig. 7. Displaying all the details in a Graph for given range

Fig. 8. Displaying all the details and Holzer tables for given range

Further proposed algorithm facilitates to change the selected range of the graph to observe data closely as shown in Fig.9.

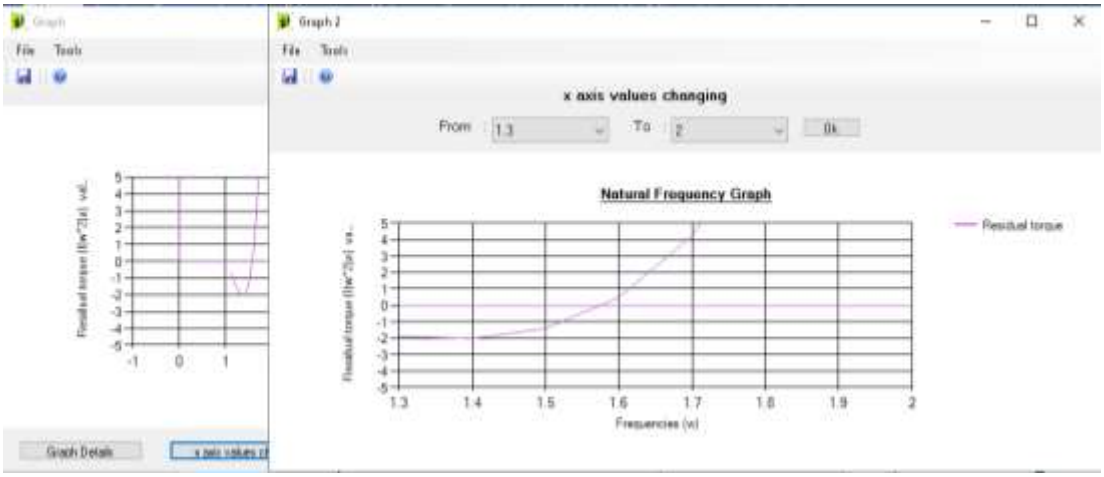

Fig. 9. Changing the range of the frequency

C. The graphs can be plotted with different parameters.

From this proposed software we can obtain necessary parameter values by changing parameters for the given range. As shown in Fig.10 Holzer tables and graphs can be obtained according to the range of frequency(ω^2).

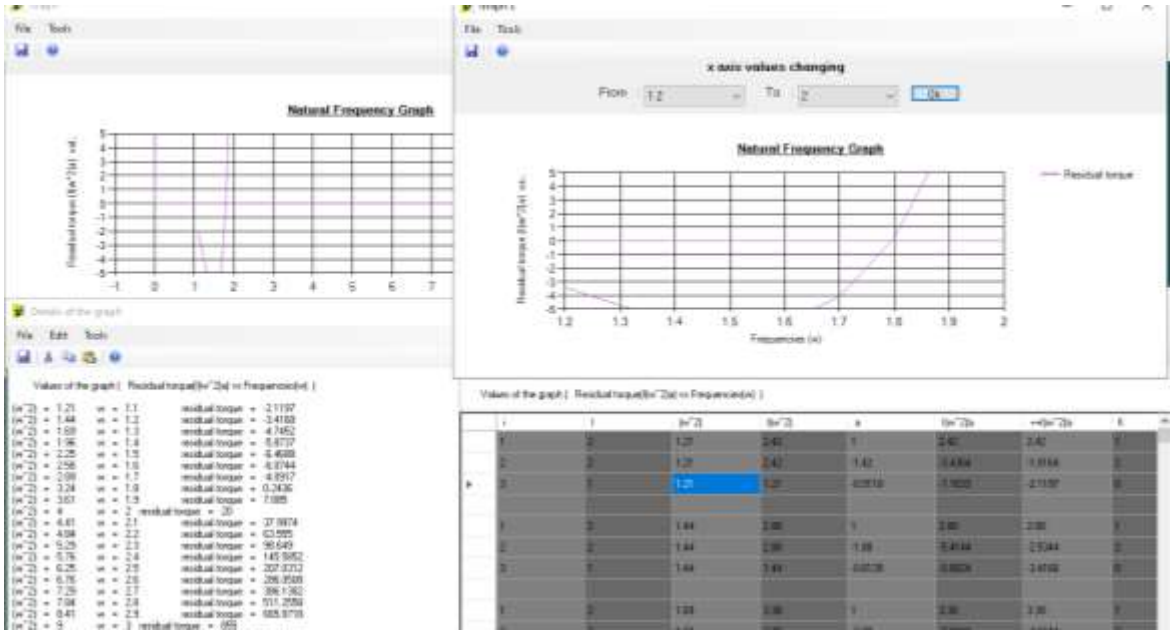

Fig. 10. The details, Holzer tables and graphs according to the range of frequency(ω^2)

As shown in Fig.11 Holzer tables and graphs can be obtained according to the range of moment of inertia (I).

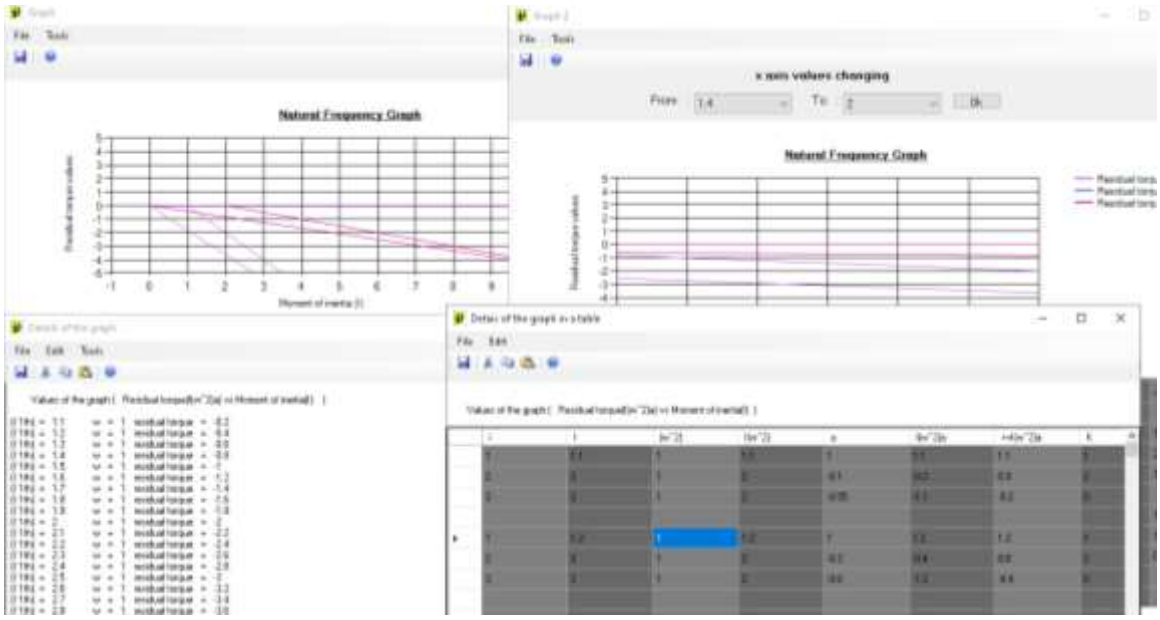

Fig. 11. the details, Holzer tables and graphs according to the range of moment of inertia (I)

As shown in Fig.12 Holzer tables and graphs can be obtained according to the range of diameter and length of shaft.

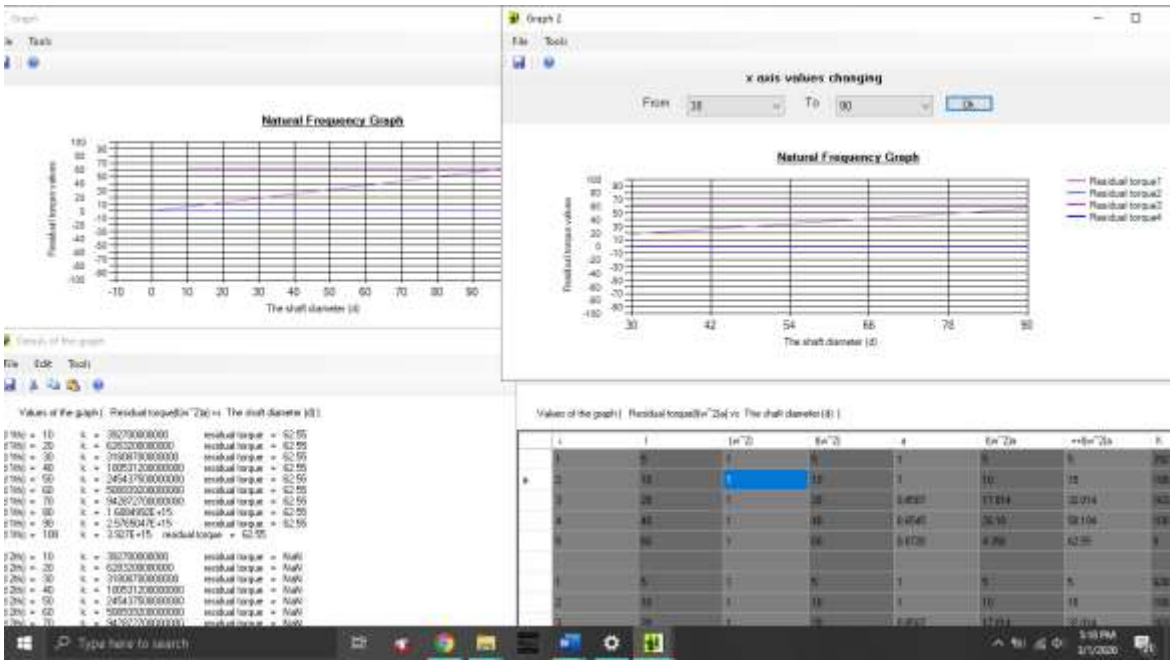

Fig. 12. The details, Holzer tables and graphs according to the range of diameter and length of shaft

D. This proposed software facilitates to save all the tables, graphs, and other details in any format.

4 CONCLIUSIONS

In this study we developed an algorithm to facilitate torsional vibration with multi degree of freedom. In industry there are different types of torsional vibration systems and for the performance and stability of such systems, vibration is directly affected. When vibration amplitude increases significantly, that could lead to catastrophic failures. Therefore, the system should be modified to drive the shaft with a suitable motor frequency according to the application, which leads to minimum risk of failure. The important parameter is the Natural Frequency of the system and it should be calculated with a high accuracy. Performing manual calculation is a tedious process where repeating of calculation involves and hence time consuming. When the number of rotors exceed than three it becomes extremely difficult to determine Natural Frequency by manual calculations. This proposed algorithm facilitates to find Natural Frequencies in straight line free or forced torsional vibration systems and one end fixed systems. The proposed algorithm is capable of calculating Natural Frequency faster and accurate.

In future it is expected to develop the algorithm to accommodate systems with torsional vibration of a branched system, forced torsional vibration of a branched system, torsional vibration of a branched one end fixed system, forced torsional vibration of a branched one end fixed system and damped torsional systems.

REFERENCES

Quiroga. J., Bohórquez. O., Ardila. J., Bonilla. V., Cortés. N. and Martínez, E. (2019). *Torsional natural frequencies by Holzer method*. Journal of Physics: Conference Series. 1160. 012008. 10.1088/1742-6596/1160/1/012008.

Purification of urban storm water of curb inlets using biochar embedded bio - geo filter

A A S M Priyasanka[1], B C L Athapattu[2*]

[1]Department of Civil Engineering, CINEC Maritime Campus. Malabe, Sri Lanka.

[2]Department of Civil Engineering, The Open University of Sri Lanka, Nawala, Nugegoda, Sri Lanka

*Corresponding Author: email: bcliy@ou.ac.lk, Tele: +9411288111

Abstract *– Curbs which have immerged with the development of roads have let the collected water of carriage ways to rush off from the road pavement to the line drains and then to the nearest water bodies. The water which flows may contains many pollutants with oil and grease, hydrocarbons mainly such as Cu, Pb, Ni & Zn. Thereby those get mixed with water bodies and. Therefore, this research was aimed to develop a model to purify urban storm water of curb inlets using bio retention filters prior it enters urban water bodies. The prototype was developed by using water from an urban canal hypothesizing that its water accumulated through curbs. A prototype of the bio char embedded bio-geo filter was designed and developed for treating the water varying the loading rate. Accordingly stream water initially was let to flow over biochar embedded grass strips and by changing loading rate, optimum flow velocity was obtained for designing roadside curb inlet and the bank of the urban stream bank. The proposed system successfully removed organic, inorganic, and heavy metals from storm water, which can be applied for purifying storm water of the roadside curb inlets with an appropriate design.*

Keywords*: Bio-Geo filter; Urban storm water; Curb inlets; Heavy metals; Biochar*

1 INTRODUCTION

Recently Sri Lanka has been subjected to industrialization. As a result prevailing high traffic condition has become a serious challenge in transportation sector. Accordingly, the road network has been subjected to expansion for reducing traffic. However, the unnoticeable fact is that many types of pollutants, which originate from variety of sources, accumulate specially over the road surfaces. Due to increase of impervious land area, storm water runoff of urban areas has become a severe threat on the environment and aquatic ecosystems during the rainy season. Therefore, it is essential to introduce a proper way to treat storm water without letting flow into natural surface water bodies directly.

Storm water runoff contains solid wastes, road sweeps, hydrocarbons, sand, silts and other particulate matters which can be chemical, physical or biological (Erickson *et. al*, 2013). Among those, the major influence is the habitat alteration and biological integrity due to loading sediments, chlorides, heavy metals, nutrients, and biological oxygen demanding substances of water.

Roads and highways consist of micro pollutants such as hydrocarbons & heavy metals which combine with sediment particles (Aryal *et. al*., 2005). Usually in storm water runoff contains wide range of organic compounds such as hydrocarbons produced in combustion process (Kennedy *et. al.,* 2016; Huber et al., 2016). Arsenic (AS), Cadmium (Cd), Chromium (Cr), Cobalt (Co), Copper (Cu), Lead (Pb), Nickel (Ni), Zinc (Zn) were founded as the crucial contaminant metals in the storm waters due to their toxicity, and lack of degradability (Kennedy *et. al.,* 2016). Due to long-time dry periods, accumulation percentage of those pollutants may also increase and with rainfall, those washed out to the water resources while polluting water resources (Wang *et. al*., 2017).

Wetlands are the most important eco-system on the earth due to its unique hydrologic conditions and connection between terrestrial and aquatic systems (Brix, 1994). But in the present days, wetlands are reclaimed to build residents or drained for agricultural purposes. Therefore, the reduction of natural wetland causes to build up artificial bio retention ponds. Retention ponds or wetland concepts have been developed as a sustainable solution for the treatment of the storm water runoff with the ability of flood potential reduction and water quality enhancement. Integration of pollutant absorbents such as vegetative diversity and geo-materials reinforce the water purification process by facilitating the biogeochemical reactions. Bio char is a by-product of thermal decomposition of wood, plant leaves and such organic matters are under a limited substances environment below 700^0C. Bio char contains more than 60% of carbon and is used as a soil amendment material (Igalavithana *et. al.,* 2017). It can be used as a microbial inoculants carrier and as a water treating agent (Gwenzi, et al., 2017). Due to its high surface area and oxygen containing surfaces, it can adsorb heavy metals and inorganic compounds such as nitrates and phosphate. The removal of phosphate from water using bio char limits the eutrophication impact on natural water ways. Saw dust bio char has been found to be effective in wastewater improvement (Lou et al., 2016; Kitchener 2017).

In this context a remedial model to treat the storm water runoff on road pavements was introduced as pollution control systems to enhance water quality of urban drainage canals. Therefore, this research was focused to characterization of curb storm water and to introduce purification system using an urban storm water by using biochar embedded bio-geo filter.

2 METHODOLOGY

2.1 Demarcation of sampling points

Storm water from curb inlets were collected on the road pavement area for characterizing the curb water. Turbidity was measured using HACH 2100P Turbidity meter while pH was measured using JENWAY 3510 pH Meter. Electrical conductivity and temperature were measured using JENWAY 4520 Conductivity Meter while NO_3 and PO_4 were measured using HACH DR 900 Colorimeter. For COD measurements the samples were digested using HACH DRB 200 and then measured using HACH DR 900 Colorimeter. The samples were digested for heavy metal measurements and then measured using ICP-MS.

2.2 Setting up the Experimental model for treating curb storm water

Plywood board of size 2000mm x 500mm was placed forming a gentle gradient of 7:1. Bed of the plywood was fully covered with polythene and a frame was fixed around the plywood of 8cm height.

Biochar was produced by pyrolyzing Gliricidia biomass at <700 ^{o}C in a closed reactor as a by-product of generating energy (Athapattu et al, 2017). Kabook used for this experimental set up was obtained from a demolished house as a waste construction material. Bio char and Kabook was selected 6.35 to 4.76 mm after the sieve analysis and mixed in the volume of 3:1. Mixed bio char and Kabook was layered on the prepared plywood board and sealed them tightly with a use of chemically inactive net. A grass layer was grown over the biochar bed and allowed to grow for few weeks prior to the experiment. Inlet was prepared to shower the water from a higher elevation. A PVC pipe of length 500mm was drilled with hole 1mm diameter with 5mm intervals and fixed horizontally to distribute the water equally along the grass layer. A 500 L tank was setup and flowrate were controlled and fed the system. It was assumed that the urban canals collect road sweeps and storm runoffs during the rainfall and therefore the urban canal water contains considerably higher concentrations of pollutants. The distilled water obtained was used as the datum for inland surface waters.

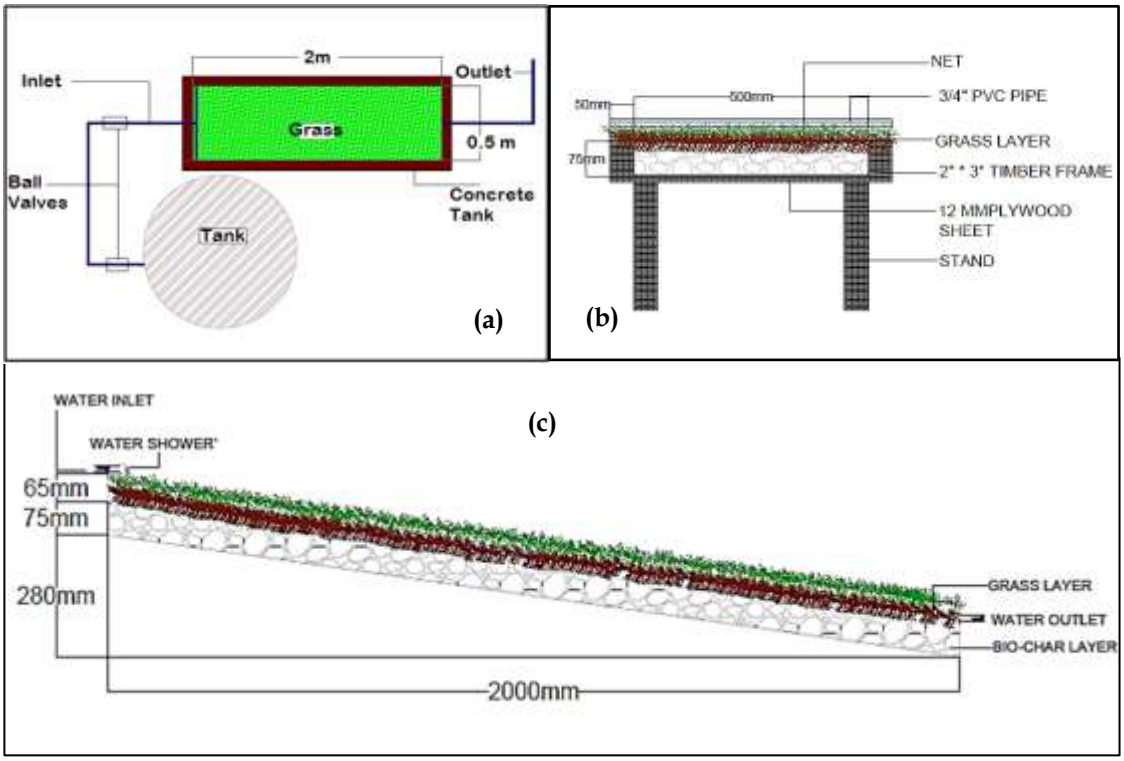

Fig. 1: Details of biochar embedded bio geo filter excremental setup
(a) Plan View (b) Elevation (c) Longitudinal section

The periodically collected samples from inlet and outlet of the experimental setup were measured to estimate the removal efficacies. Fig.1a, 1b and 1c are shown the plan view, elevation, and longitudinal section of the experimental set of biochar embedded bio geo filter, respectively. Fig. 2 shows the pictorial view of model set up at the laboratory. Initially, fresh water was flow over to wash out the system. After cleaning the setup, storm water was filled to the overhead tank and allowed to run with different flow rates such as 10mls^{-1}, 20mls^{-1}, 30mls^{-1}, 50mls^{-1} and 100mls^{-1}. Flow rate was measured while controlling the valve and used to fill a known volume within a known retention time. Drain outs were collected after saturating the bio char and Kabook layers. The drain out

samples were tested for turbidity, total suspended solids (TSS), chemical oxygen demand, electrical conductivity, nitrates, phosphates, pH and for selected heavy metals.

2m long, 0.5m wide and 0.075m high grass buffer was prepared for the treatment process. The total volume of the wetland is $0.075m^3$. $1/4^{th}$ total volume was filled with Kabook and ¾ volume was filled with sieved bio char. Water inlet and outlets were made by installing ¾" PVC pipe and placed horizontally to the supply pipe. Assuming the storm water level in the tank is constant the saturation time was calculated and allowed to saturate.

Fig. 2: Pictorial View of Wetland Model

3 RESULTS AND DISCUSSION

Water quality parameters of storm water coming out from the curb inlets are shown in Table 1. The average water quality of storm water was estimated using three different rainfalls obtained monthly for three months. The monthly rainfall of said consecutive months were 50mm, 315mm and 117mm.

Table 1: Characteristics of storm water of curb inlets at Metro city, Sri Lanka

Parameter	value
Temperature ^oC	30±2
Turbidity (NTU)	28.7±8
Conductivity (µs/cm)	71±24
TSS (mg/L)	11±3
Oil & Grease	0.7±0.3
pH	8.8±0.4
COD	72±35
Nitrate (mg/l)	1.1±0.4
Phosphate (mg/l)	0.35±0.5
Zn (mg/l)	0.369±0.005
Pb (mg/l)	0.042±0.002

It was noted that high turbidity can be observed with the high rainfall intensity. This occurs due to increasing of TSS in the storm water runoff. With the minimum intensity of rainfall, turbidity increases while turbidity decreases during medium rainfall intensity. Total suspended solids (TSS) shows considerable fluctuation while lowest TSS value was recorded as 9 mg/L during the moderate rain.

However, it also varies with the sample time and the location. Usually organic contaminants may increase the amount of TSS along roadsides. Oil and grease content of storm water sample was considerably higher during high rainfall intensity. Storm water run-off was almost alkaline however frequent raining makes it towards acidic.

The maximum electric conductivity was recorded as 114.5µs/cm. However, electric conductivity of fresh water fluctuates from 15 – 30 µs/cm. with moderate and lower conditions of raining it may deviate a little. Chemical Oxygen Demand also varies with the rainfall intensity. It fluctuates from 46mg/l to 91mg/L. during the period of concern. However, it was observed that, the minimum of COD of storm water was considerably higher than freshwater COD (10 mg/l). Further, 1.5 mg/l of nitrates was observed while lowest nitrate, 0.8 mg/l was observed during mild rainfall. Hence the heavy rain conditions, nitrate may dilute with runoff. In fresh water it was recorded as 0.08 mg/l of nitrates.

Phosphates showed the similar variation as nitrates. Minimum value of 0.28 mg/l is seen in high rainfall intensity due to the dilution of contaminants. However, in freshwater phosphate concentration was nearly 0.07 mg/l. Usually of 0.002 mg/l of zinc recorded in fresh water while the storm water showed considerably higher value. In addition, lead concentration of fresh water (<0.001 mg/l), while the storm water Pb value deviate considerably probably due to vehicle emissions.

3.1 Removal of pollutants through the system

The experimental setup was initially fed with fresh water for 24 hrs to saturate the system. Thereby runs were repeated with different loading rates and water quality parameters were measured with respect to the initial sample parameter. The Table 2 shows the pollutant removal efficiency when passing through the biochar embedded bio geo filter system.

Table 2: Pollutant removal efficiency of stormwater using purification system

Experiment Series	Influent Loading Rate	Percentage removal								
		Turbidity (%)	TSS (%)	pH (%)	COD (%)	Electrical Conductivity (%)	Nitrate (%)	Phosphate (%)	Zn (%)	Pb(%)
Run 1	10 ml/s	45.50	30.00	4.40	43.24	1.32	76.56	2.22	69.64	55.38
Run 2	20 ml/s	60.27	30.00	6.59	45.95	7.05	76.56	38.52	68.58	46.15
Run 3	30 ml/s	60.32	30.00	4.40	40.54	5.29	67.19	40.00	66.00	38.46
Run 4	50 ml/s	63.60	30.00	3.30	35.14	7.93	64.06	42.96	59.44	23.08
Run 5	100 ml/s	63.92	30.00	17.58	0.00	8.37	39.06	47.41	33.41	6.15

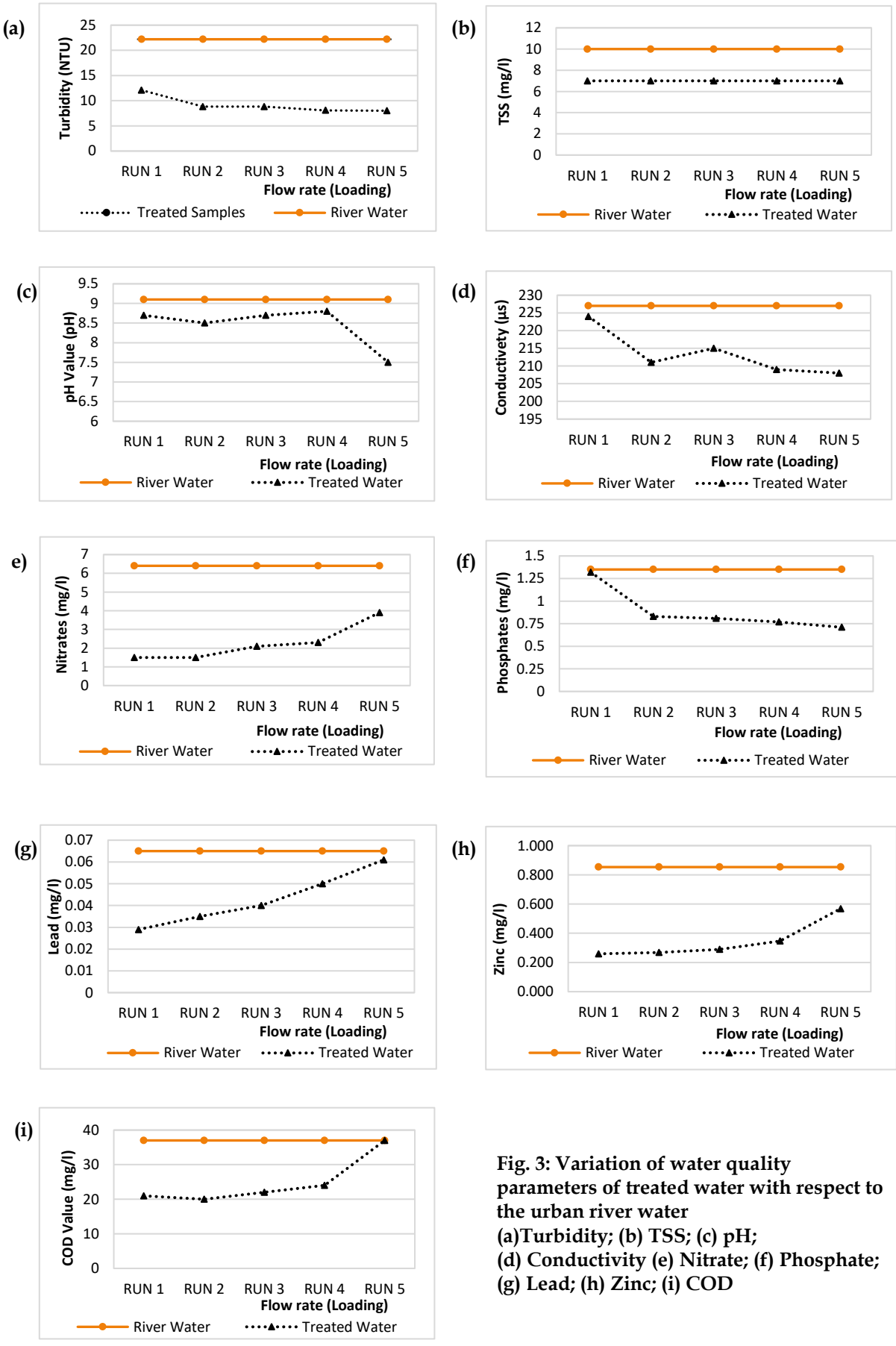

Fig. 3: Variation of water quality parameters of treated water with respect to the urban river water
(a)Turbidity; (b) TSS; (c) pH;
(d) Conductivity (e) Nitrate; (f) Phosphate;
(g) Lead; (h) Zinc; (i) COD

Fig. 3 shows the removal of respective contaminants when passing through the experimental biochar embedded bio geo filter. A reduction of turbidity is clearly seen with respect to the initial turbidity. COD was varied with the initial value in every run. Minimum COD value was observed in RUN 2 and maximum value was observed in RUN 5. But the Electric conductivity is gradually decreased with the increase of flow rate. Minimum obtained value is 208 µs/cm. Total suspended solids were constant (7mg/l) in every run and it was minimized from the original value. The treatment of nitrogen has been decreased with the higher loading rates. Maximum treatment was occurred at the RUN 1 and minimum Treatment was occurred at RUN 5.

Phosphate removal was enhanced by the system however regular increment can be seen. Minimum treatment was occurred in the RUN 1 while maximum treatment had occurred in Run 5. When consider the removal efficiencies of heavy metals; Pb and Zn showed considerable removal efficiency however the Zn removal efficiency is considerably higher than the Pb. With the increment of the water flow rate, the treatment percentage decreased gradually. With respect to the above percentages, the treatment process on the RUN 2 had the highest treatment efficiency of 42 % total.

3.2 Application of the curb water purification system

The elevational heights of the roadside or any topographical changes of the area can consider for this application. Fig. 4 is shown a proposed application with relevant elevations of the ground and a water flowing structure. Accordingly, the existing slope should be gentle slope for better filtration process. The grass buffer with bio char is to be applied with a gradient of 1:7 towards a horizontal distance of 3.0 m. At the end, a concrete drain of 600 mm x 500mm of gradient 1:100 is to be constructed to transfer the treated water to a retention pond through the grass buffer. The retention pond shall construct with integration of bio geo-materials.

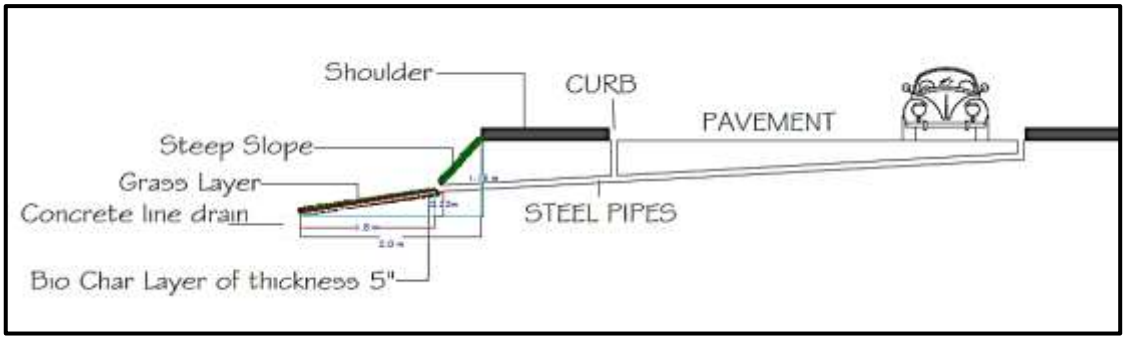

Fig. 4: Illustration of setting out stormwater treatment system at the curb inlet

4 CONCLUSION

This study was conducted for the storm water to clarify the impurities associated. Several parameters, Zn, Pb, NO_3^-, PO_4^{-2}, oil and grease, suspended solids, turbidity, COD, pH, electric conductivity were checked by changing loading rate. The flow measurements were taken from the inlet and the outlet of the bio char embedded bio-geo filter while increasing the loading rate from 10ml/s to 100ml/s. The concentrations of effluents were

measured to investigate the removal efficiency of the system which simulates the roadside curb inlets.

According to the removal efficiency, a maximum efficiency was shown in 20 mls^{-1} loading rates. Minimum was obtained with maximum flow rate of 100mls^{-1} proving the heavy rainfall intensities will drastically impact on road sweeps to the nearby water ways. In this experiment, it was used only a 75mm bio char layer and it was treated using a fixed gradient of 1:7. This can be varied according to the topography of the available land. As 20mls^{-1} have shown good removal efficiency and it deviates with the gradient, application length and thickness to the bio char layer the practical application can be adjusted accordingly to obtain the better removal rate.

Though the maximum efficiency of the bio char layer for flowing water is 42%, if it be retained, the efficiency is much more than the above. Therefore, bio char can be used as a treatment agent for storm water enhancing and it can be easily applicable to the roadside curb inlets with a greening strip before flowing into the nearby urban canals. Such green application will bring the sustainable built environment to harmonize with the urbanized activ*iti*es.

REFERENCES

Aryal, R.K., Jinadasa, H.K.P.K., Furumal, H. and Nakajima, F. Long Term Suspended Solids Run off simulation in Highway Drainage System. (2005) *Water Science & Technology*, Vol 52 No 5 pp 159–167.

Erickson, A.J., Weiss, P.T. and Gulliver, J.S. (2013) Optimizing Stormwater Treatment Practices. *A Handbook of Assessment and Maintenance*, DOI 10.1007/978-1-4614-4624-8_2

Athapattu, BCL., Thalgaspitiya, TWLR. Yasaratne, ULS., and Vithanage, M. (2017) Biochar- based constructed wetlands to treat reverse osmosis rejected concentrates in chronic kidney disease endemic areas in Sri Lanka. *Environmental Geochemical Health*, 39 (6), pp 1397-1407 DOI: 10.1007/s10653-017-9931-8

Brix, H. (1994) Use of Constructed Wetlands in Water Pollution control: Historical Development, Present Status, And Future Perspectives. *Wat. Sci. Tech.,* Vol.30, No.8, pp. 209-223

Ellis, B., Revitt, M., Shutes, R.B.E. and Kingley, J.M. (1994) The performance of vegetated bio filters for highway runoff control. *Science of The Total Environment*, 1994:543-550

Gwenzi, W., Chaukura, N., Noubactep, C. and Mukome, F N. D. (2017) Biochar-Based Water Treatment Systems as a Potential Low-cost and Sustainable Technology for Clean Water provision in Developing Countries. *Journal of Environmental Management*. 2017 Jul 15;197:732-749. doi: 10.1016/j.jenvman.2017.03.087.

Huber, M., Badenberg, S, C., Moritz, W., Drewes, J. E., and Helmreich, B. (2016) Evaluation of Factors Influencing Lab-Scale Studies to Determine Heavy Metal Removal by Six Sorbents for Stormwater Treatment, *Water* 2016, 8, 62; doi:10.3390/w8020062

Igalavithana, A. D., Mandal, S., Niazi, N. K., Vithanage, M., Parikh, S J., Mukome, F. N. D., Rizwan, M., Oleszczuk, P., Wabel, M A., Bolan, N., Tsang, D. C. W., Kim, K H. and OK, Y S. (2017) Advances and future directions of biochar characterization methods and applications. Environmental *Science and Technology 2017*, *Vol*. 47, No. 23, 2275–2330.

Kitchener, B.G.B., Wainwright, J. and Parsons, A.J. (2017) A review of the principles of turbidity measurement. *Progress in Physical Geography*, 41 (5). pp. 620-642. ISSN 0309-1333

Lou, K., Rajapaksha, A.U. Oak, Y S., Chang, S X. (2016) Pyrolysis temperature and steam activation effects on sorption of phosphate on pine sawdust biochar's in aqueous solutions. *Chemical Speciation & Bioavailability*, Vol . 28, No . 1-4, 42–50.

Navamani, S.R., Jayananda, H.T.H.L., Fernando, W.B.D.T., Rizny, M.A., Amarathunga, T., Weragoda, W.A.K.D and Miguntanna, N.P. (2015) Analysis of first flush of roof runoff and wash off process of the different roofing materials. *5th International Research Symposium on Engineering Advancements (RSEA-2015)*, 2015 Apr 25,Malabe, Sri Lanka. 2015. p. 110-6.

Kennedy, P., Allen, G and Wilson, N (2016). The management of hydrocarbons in stormwater runoff: a literature review. Prepared by Golder Associates (NZ) Limited for Auckland Council. Auckland Council technical report, TR 2016/010

Wang, J, Zhao, Y., Yung, L., Guangpeng X. and Fand, Xing (2017) Removal of Heavy Metals from Urban Stormwater Runoff Using Bioretention Media Mix. *Water 2017*, 9, 854; doi:10.3390/w9110854.

Zumrawi, M. M.E. (2014) The Impact of Poor Drainage on Road Performance in Khartoum. *International Journal of Multidisciplinary and Scientific Emerging Research*, ISSN – 2349-6037, Vol.3, No.1(October 2014).

Journal of Engineering and Technology
of The Open University of Sri Lanka (JET-OUSL), Vol. 7, No.2, pp. [31-43], 2019

Performance Improvement of Biomass Fired Thermic Fluid Heaters Used in Sri Lanka

Y. Priyankara, N. T. Medagedara*

Department of Mechanical Engineering, The Open University of Sri Lanka, Nawala, Nugegoda, Sri Lanka

*Corresponding Author: tmmed@ou.ac.lk, Tele: +94112881113

Abstract – *The best industrial heating solution depends on the type of application. Heaters are used in different applications in many industrial settings. Industries such as plastic, food, oil, gas and the chemical industry all use industrial heaters (oil, gas, electric, and biomass) in various processes. Electric heaters are good enough for small applications due to high cost of the electricity. Sometimes it is used as stand-alone units where the equipment cannot be installed close to the main heat source. Steam boilers too are used in Sri Lanka for many heating applications. Hot fluid heaters are also used, but not as much as steam boilers. Moreover, biomass is widely used in Sri Lankan industry for heating requirements due to high furnace oil prices. Many people use a water heater instead of a boiler for radiant floor heating because of less cost. A thermic fluid system is similar in nature to the hot water boiler system and this fluid can be heated up to 300 ^{0}C under low pressure. Thermic fluid heater is a unit in which a liquid phase heat transfer medium is indirectly heated and circulated to one or more heat energy users within a closed loop system.*
This paper discusses about the performance enhancement of the biomass fired thermic fluid heater installed in a company located in Malwana, Sri Lanka. This company mainly manufactures rubber gloves which does not require high pressure but require high temperature. Low efficiency, high energy consumption and high stack temperature are the main problems of the plant. This study showed that by optimizing the plant parameters, the total heat loss can be reduced from 58% to 25%, hence the overall efficiency of the plant can be increased from 42% to 70%. Results were verified by using Engineering Equation Solver (EES) software.

***Keywords**: Thermic fluid heaters, Boilers, Biomass*

Nomenclature

M - mass of fuel burnt (kg/h)
C - Calorific value of saw dust (kCal/kg)
$\dot{v}$ - Volume flow rate (m^3/h)
$\Delta\theta$ - Thermic fluid inlet and outlet temperature difference (^{0}C)

c - Specific heat (kCal/kg^{0}C)
ρ - Density of the thermic fluid (kg/m^3)
k - Heat transfer efficiency factor (W/m^{2}K)

1 INTRODUCTION

The share of biomass consumption in the total energy demand is 45.4% in 2017, whereas the share of petroleum was 43.1% (Sri Lanka Energy Balance, 2017). Boilers are mainly used in Sri Lanka for heating requirements in the industry. Biomass are mostly used in boilers and it is estimated that the biomass usage in industrial sector is 75.8% in 2016 while 78.4% in 2017 (Sri Lanka Energy Balance, 2017).

Fuelwood are the most common forms of biomass (Abeywardhena, 2005). There are other heating methods such as hot fluid heaters, but the usage is less compared to boilers. Use of steam for heating applications are essential for some applications like steaming rice in the process of parboiling, heating, and pressurizing of tyre moulds in tyre manufacturing process.

Thermic fluid heater is industrial heating equipment, used where only heat transfers are desired instead of pressure. A thermic fluid is circulated in the entire system for heat transfers to the desired processes. The heaters are used in curing ovens, tank heating, autoclaves, calendar mills, die-mould heating, building heating systems. Thermic fluid heaters are also used for curing of rubber gloves or as heat exchangers which is not required high pressure but need higher temperature. Usage of biomass fired thermic fluid heaters are rapidly growing in the industry. Though thermic fluid heaters considered as high-tech or easily adoptable, the installations are limited due to lack of awareness, minimal guidance and also jurisdictions are low for regulating thermic fluid systems [Omer, 2008].

Use of suitable heating source for an application in industrial context is vital as it gives huge economic benefits. Nowadays the thermic fluid heaters become emerging technology for heating solutions for industrial application in Sri Lanka because of its advantages over steam boilers. Main advantages of the thermic fluid heaters are less operational and low maintenance cost. High temperature under low pressure is another advantage over steam boiler because of higher safety related accident reported with steam boilers.

Thermic fluid heaters are in two forms based on the primary energy source, namely furnace oil and biomass. Biomass fired thermic fluid are less popular because of higher fuel price. Still there is abundance of biomass available and considered as sustainable energy source in Sri Lanka (Rathnasiri, 2008). Therefore, this research is focused on the performance enhancement of 3MkCal/h thermic fluid heater and the method of analysis adopted can be replicated to any thermic fluid heater, which is categorized under thermic fluid heaters. In addition, it is also aimed to provide recommendations for poor plant efficiency, higher consumption of biomass and higher stack temperatures that are identified as the main problematic issues of the plant. Therefore, identifying drawbacks of the existing system and conducting a theoretical study for optimizing the system performance by using thermic fluid were the main objective of this research.

1.1 Biomass Fired Thermic Fluid Heater

Thermal fluid heater (TFH) is a unit which uses the indirect heating, in which a liquid phase heat transfer medium is heated and circulated to one or more heat energy users

within a closed loop system. The common heat transfer media are thermic oil, glycol, and water (Devraja et al, 2019) . Nevertheless for common thermic fluid heaters (TFH), the working fluid is thermic oil. The process of the thermic fluid system is similar to the hot water boiler system. This fluid can be heated up to 300 ^{0}C under low pressure which is beneficial for processing of the system.

There are many advantages of having thermic fluid heating system over steam boiler. In thermic fluid heating systems, there are no corrosion in pipes and fittings as there is no water circuit in TFH. This system has simple piping circuit with free from blow down/steam traps and no water treatment required. Furthermore high temperature under low pressure, less maintenance, less operating cost, no fluid losses and hence no fluid make-up required, heating and cooling with a single fluid, new additions are easy to incorporate are the wealth of using thermic fluid heating systems (Wadkinson, 2012).

Steam is an excellent medium for energy transfer, but it is much expensive to use due to the cost associated with operation, maintenance in the today's context (Wanson, 2008). The water treatment activities, frequent inspection and blow downing are required during operation of a boiler. In addition to that, the maintenance of steam traps and valves, frequent tube cleaning and inspection cause the higher operational and maintenance cost. Thermic fluid heater provides less cost during operation and maintenance comparing to the steam boilers. For smooth operation of the system the performance can be further enhanced with periodic cleaning of the coil unit and general preventive activities such as greasing.

Basically, the installation cost is almost same for an equivalent capacity biomass fired boiler and a thermic fluid heater excluding pre and feed water treatment facilities of a boiler. Piping circuit installation cost for steam boiler is higher due to stainless material used for piping. Additionally, a thermic fluid heater piping circuit is required for thermic oil filling-up which cost substantial amount of initial cost.

The risk associated with the steam boiler hazards is one of the main aspects on research alternatives. The most common boiler hazards that lead to accidents are low water levels, excessive pressure, and a failure to purge combustible gases from the firebox before ignition. These hazards can cause serious boiler accidents like explosions or fire. In addition to boiler accidents the economic loss which has raised increasing concern to take measures against awareness of installation and operation of boilers (Prinyankara & Medagedara, 2016; Bierl, 2017). No such explosions can take place in TFHs since it is operating below 2 bar pressure. Therefore, lower safety risk is one of the biggest advantages that thermic fluid heater has over steam boiler.

1.2 Main Features and Operation of Biomass Fired Thermic Fluid Heater

The operational system of vertical biomass fired thermic fluid heater (Thermax 2013) is shown in figure 01. Normally the combustion chamber of the furnace is designed to get the required amount of heat capacity of the heater. Heat transfer happens through both convection and radiation. The number of heat exchangers depend on the requirement of the heat capacity of the plant. Fuel used in thermic fluid heaters are furnace oil, gas, coal or biomass such as wood chip (WC), saw dust (SD), briquettes or pellets. Biomass is widely used in Sri Lanka due to relatively higher furnace oil prices. But the preparation of the fuel is required when using biomass like wood chip or saw dust. Moisture is a critical factor,

because increase in moisture from 0% to 40% may decrease the heating value by about 66% as some literature reveals.
Thermic fluid heater is also provided with forced draft fan, induced draft fan to control the air draft inside the combustion chamber. An Air pre-heater is used for air pre-preparation for combustion with the help of flue gas. When the combustion process is over this flue gas is expelled through the smokestack. In the thermic fluid heater, the flue gas is passed through air pre-heater, water pre-heater, pollution control unit before it is expelled to the environment. Forced draft fan and induced draft fan are controlled in such a way that negative pressure is kept inside the combustion chamber all the time. Therefore, this achieves good combustion as this allows fuel to mix with air rather than resting at the bed.

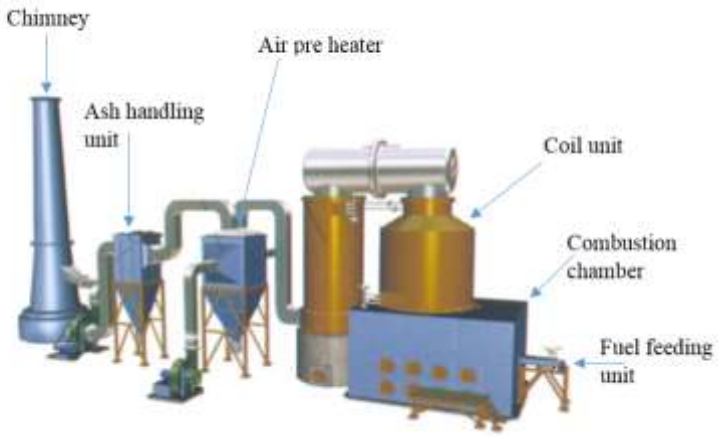

Fig. 01: Vertical biomass fired thermic fluid heater (Thermax, 2013)

As figure 01 shows the coil unit absorbs the heat from flue gas and delivers to the heat exchangers located at heat demand points through the piping circuit where heat is used for effective use. (Sigma Thermal, 2016). Piping circuit is a closed system and therefore there is no fluid losses. But it is opened to the atmosphere at the expansion tank to cater to the fluid volume variations during temperature increment.

1.3 Performance Parameters of Thermic Fluid Heaters (TFH)

Attributes of the performance of a thermic fluid heater are outlined as fuel consumption combustion performance, heat transfer performance and flue gas handling. Fuel consumption is a main design parameter for TFH as it mainly depends on the limitations of the fuel limit to attain the required heat. In the case of biomass, fuel consumption depends on the size of the fuel particles, moisture level, fuel damper adjustment, air draft pattern and absence of debris in the fuel.

The level of the quality of the fuel and air handling are the determinant factors for combustion performance. Combustion efficiency will be lower when using fuel which has higher moisture level, bigger size chips and presence of foreign particles. In addition, combustion efficiency will be lowered if the air flow is not uniformly spread throughout the combustion chamber. Improper combustion not only reduces efficiency but also increases fuel consumption and environment pollution.

Heat received by the thermic oil depends on the quality of the thermic oil, oil flow rate and the temperature difference ($\Delta\theta$) in fluid inlet and outlet pipes. The characteristics of the pipe and its material are also affected by the heat transfer rate.

1.4 Optimizing the Heat Transfer Performance of TFH

Performance optimizing is referred to as running of TFH within designed limits. Therefore, identification of accurate heater efficiency and opportunities for efficiency improvement are estimated for thermic fluid plant as well. Performance of the plant is characterized by its efficiency level. For the calculation of boiler/heater efficiency, direct and indirect methods can be used.

1.4.1 Direct Method

This is a common method of calculating boiler/or heater efficiency. It is the percentage ratio of heat received by the working fluid to the heat supplied by the fuel.

$$\text{Efficiency } (\eta) = \frac{\text{Heat received by the working fluid x 100\%}}{\text{Heat supplied by the fuel (SD)}} \quad \text{----------(i)}$$

1.4.1.1 Heat Supplied by the Fuel (Saw dust)

$$\text{Heat supplied} = M * C \quad \text{----------(ii)}$$

Where M – mass of fuel burnt (kg/h)
C – Calorific value of saw dust (kCal/kg)

1.4.1.2 Heat Received by the Working Fluid (Thermic fluid)

$$\text{Heat received} = \dot{v} * \Delta\Theta * c * \rho * k \quad \text{----------(iii)}$$

Where
$\dot{v}$ - Volume flowrate (m^3/hr)
$\Delta\Theta$ - Thermic fluid inlet and outlet temperature difference (^0C)
c - Specific heat ($kCal/kg^0C$)
ρ - Density of the thermic fluid (kg/m^3)
k - Heat transfer efficiency factor

1.4.2 Indirect Method

This is also known as the heat loss method. The efficiency can be calculated by subtracting the heat loss fractions from 100 as follows:

$$\eta = = 100 - (i + ii + iii + iv + v + vi + vii)$$

Where the principle losses are,

i. Dry flue gas
ii. Evaporation of water formed due to H_2 in fuel
iii. Evaporation of moisture in fuel

iv. Moisture present in combustion air
v. Unburnt fuel in fly ash
vi. Unburnt fuel in bottom ash
vii. Radiation and other unaccounted losses

The governing standards with regards to the indirect method are the British Standard, BS 845:1987 and the USA Standard ASME PTC41Power Test Code Steam Generating Units.

1.4.3 Calculation of principle losses

Principal losses depend on theoretical air requirement, percentage of excess air and actual mass of air supplied/kg of fuel. Once those have been estimated, heat losses can be estimated to obtain the heater efficiency.

Theoretical air requirement = [(11.43 x C) + {34.5 x (H_2 – O_2/8)} + (4.32 x S)]/100 kg/kg of fuel ----------(iv)

Percentage of excess air supplied (EA) = $\frac{O_2\%}{21-O_2\%} X\ 100$ ----------(v)

Actual air supplied (AAS) per kg of fuel = {1 + EA/100} x theoretical air --------(vi)

1.4.5 Heat losses

(i) Percentage heat loss due to dry flue gas = $\frac{M\ X\ C_p\ X\ (T_f - T_a)}{GCV\ of\ fuel}$ x 100 ----------(vii)

C_p = Specific heat of flue gas = 0.23 kcal/kg ˚C
M = Mass of dry flue gas in kg/kg of fuel
M = Combustion products from fuel: CO_2 + SO_2 + Nitrogen in fuel + Nitrogen in the actual mass of air supplied + O_2 in flue gas. (H_2O/water vapour in the flue gas should not be considered)

M = Total mass of flue gas = mass of actual air supplied + mass of fuel supplied

(ii) Percentage heat loss due to evaporation of water formed due to H_2 in fuel

Heat loss due to evaporation of water formed %= $\frac{9\ X\ h_z\{584 + C_p(T_f - T_a)\}}{GCV\ of\ fuel}\ x\ 100$ --- (viii)
Where, h_2 = kg of H_2 in 1 kg of fuel
C_p = Specific heat of superheated steam (0.45 kcal/kg ˚C)

(iii) Heat loss due to moisture present in air % heat loss due to moisture present

in air = $\frac{M\ X\ \{584 + C_p\ (T_f - T_a)}{GCV\ of\ fuel}\ x\ 100$ ----------(ix)

Where, M = kg of moisture in 1kg of fuel
Cp= Specific heat of superheated steam (0.45 kcal/kg) ˚C
* 584 is the latent heat corresponding to the partial pressure of water vapour.

2.0 METHODOLOGY

The performance enhancement of the biomass fired thermic fluid heater was considered in this study. The selected industry mainly manufactures rubber gloves which the process does not require high pressure but high temperature. The selected plant with biomass fired thermic fluid heaters plant was designed to run over 70% efficiency, when less than 30% moisture is present in the biomass fuel. As the biomass fuel saw dust and wood chips were used. The actual overall efficiency of the plant was recorded while mapping of the temperature at various points of the plant.

2.1 System Performance

Existing system was investigated meticulously to identify the drawbacks. Data archived in log form is referred for over 3 years. Some outliers were removed, and rational data was taken for the calculations. Flue gas test and moisture test were carried out at the site. With the available data Fuel used for the existing system was investigated. Further, saw dust consumption, moisture percentage of biomass, heat delivered by the fuel and heat absorbed by the system and heat losses were calculated. Efficiency was estimated using direct method and heat loss method.

To propose the improvement of system performance a deep analysis of the entire system was carried out. Few areas of the existing system such as removing excess moisture in fuel, reducing high heat loss through the stack (waste heat), reducing the percentage of excess air supply and the flue gas temperature were critically evaluated. Based on the findings of investigations, a new system was designed to overcome the identified drawbacks of the existing system.

In addition, the hourly capacity of the plant calorific value of saw dust biomass used as the fuel, hourly requirement of saw dust biomass the plant heat usage and working pressure of the plant were measured. Recovery system of waste heat, unrecovered heat discharged through the stack and flue gas temperature were also measured.

2.2 Fuel Consumption and Combustion Performance

Since the fuel consumption was varied with the demand of the final product, demand was set out with the plant utilization, waste heat, climate condition and the fuel quality. Average value was taken scrutinizing the all governing factors.

Combustion of the fuel was taken place at the combustion chamber. Air was drawn from the bottom of the grate bar bed. Saw dust was spread into the chamber by the fuel feeder. FD and ID fans were operated such that 2 bar negative pressure was kept inside the combustion chamber. This was allowed the flue gas to escape through the stack whilst transferring heat to the coil unit

2.3 Verification of the performance of proposed system

Engineering equation solver or EES software was used for the verification of the results of the proposed system. EES can be used to find out the maximization of a given function. Hence it was helpful to determine whether the proposed system is running at its optimum efficiency or not.

Governing equation for the overall efficiency of the plant were compared with the existing performance.

The overall efficiency was given as,
$\eta = 100 - [\text{Dry flue gas} + \text{Evaporation of water formed due to } H_2 \text{ in fuel} + \text{Evaporation of moisture in fuel} + \text{Other uncountable losses}]$

3.0 RESULTS AND DISCUSSION

3.1 Plant performance

The performance enhancement of the biomass fired thermic fluid heater was considered in this study. The selected industry mainly manufactures rubber gloves which the process does not require high pressure but high temperature. The plant was designed to run over 70% efficiency when biomass fuel with less than 30% moisture is present. Saw dust and wood chips were used as the biomass fuel. However, the actual overall efficiency of the plant was below 50%.

Existing system consists of pump, combustion chamber with coil unit, FD fan, air pre heater, water pre heater, pollution control unit and ID fan. Mapping of the temperature at various points of the plant is shown in figure 02.

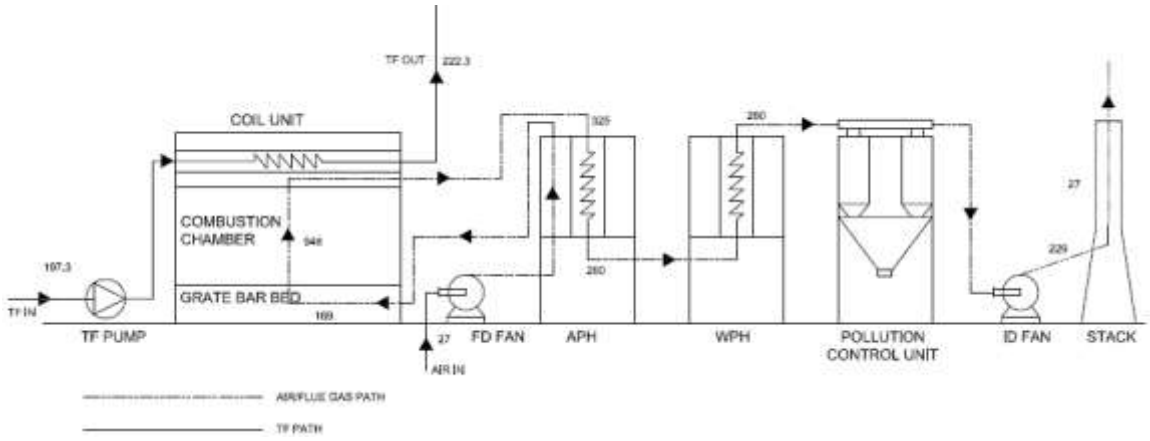

Fig. 2. Existing temperature mapping of the system

The capacity of the plant is 3million kCal/hr (12552 MJ/hr) while saw dust biomass with calorific value 2700 kCal/kg is used as the fuel. Saw dust biomass requirement is about 1.7 ton/hr with the plant heat usage is around 2.3 million kCal/hr whereas working pressure of the plant is 4 bar.

The plant is composed of a water preheater (WPH), to recover the waste heat of 0.25 million kCal/hr. This was included to generate hot water either for direct use in the manufacturing process or to run vapour absorption chiller. But unrecovered heat is discharged through the stack and flue gas temperature is above the acceptable range of 240-250 ^{0}C.

3.2 Parameters of the Existing Thermic Fluid Heating System

Quality of the thermic oil, oil flow rate and the temperature difference ($\Delta\theta$) in fluid inlet and outlet pipes and its material are fixed for a given heater and cannot be altered to increase the efficiency of the heater. The calculated efficiency of the current system was 47% from the direct calculation method and 42% from the indirect calculation method with all the losses (Table 2). The current excess air supply to the system is 180% and total heat loss is 58% as shown in table 1.

Table 1. Performance parameters of the existing system

Description	Existing set-up
Heat supplied	3,375,000 kCal/kg
Heat received	1,589,185 kCal/kg
Efficiency (direct method)	47%
Efficiency (In-direct method)	42%
Excess air supplied	180%
Total heat loss	58%
Heat loss due to moisture present	10%
Heat loss due to dry flue gas	30%
Heat loss due to H_2O formed by H_2 in fuel	15%

3.3 Drawbacks of the Existing System

Saw dust was used in this system as the biomass fuel, which was having 40% moisture content. The system preferred fuel biomass with less than 30%. However, the feeding biomass fuel was 10% higher moisture than which is preferred. Too less moisture increases fuel carry over to flue gas. Further, 10% of the heat generated is lost to evaporate the moisture present in the fuel. Efficiency of the plant is 42% whereas design efficiency is 70%. It was identified 30% of the heat is lost to the environment. In addition, no proper air circulation has occurred as grate bar bed is blocked due to saw dust particles itself. Excess air supply is 180% which is way above the preferred limit of 60%. Moreover, temperature of the air leaving the chimney is 229 ^{0}C, where design limit is 180 ^{0}C.

3.4 Proposed System for Improvement

After a thorough analysis, the few problematic areas were identified for improvements. Removing excess moisture in fuel, reducing high heat loss through the stack (waste heat), reducing the percentage of excess air supply and reducing flue gas out temperature are the focused areas to improve the performances. Accordingly, a new system was designed as shown in Fig. 3.

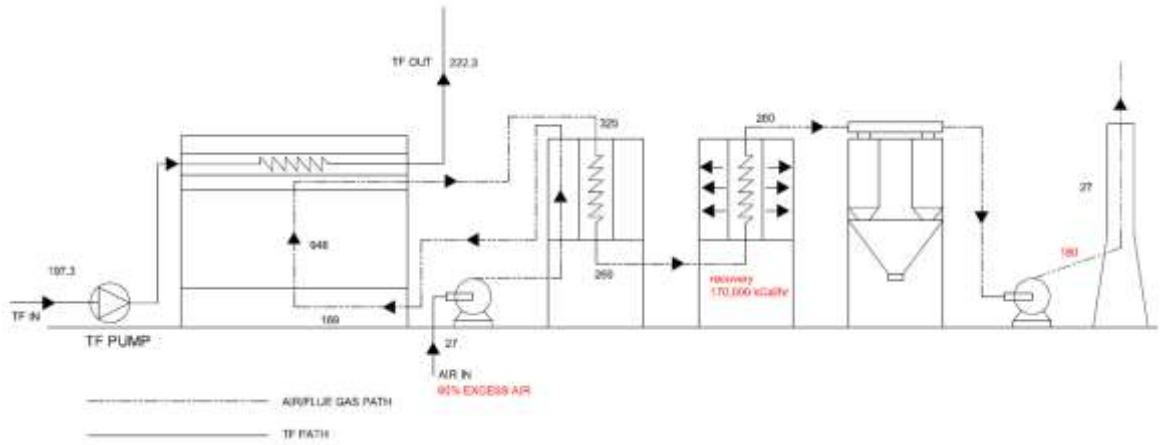

Fig. 3: Proposed Mapping of the System with Temperature Mapping

3.5 Theoretical Analysis

Proposed system suggested to recover the waste heat of 170,000 kCal/hr heat through functioning of WPH. WPH inlet and outlet is to be maintained at 260 ^{0}C and 180 ^{0}C respectively. Pre prepared saw dust is available in briquette form with 10% moisture was used for the new system. In addition to WPH is provided to recover the excess heat of the flue gas.

Performance of the new system is worked out by using indirect method and for the preferred parameters. Comparison of existing vs proposed system parameters are shown in Table 2.

Table 2. Comparison of existing vs proposed system parameters

Description	Existing set-up	New system
Heat supplied	3,375,000 kCal/kg	3,325,500 kCal/hr
Heat received	1,589,185 kCal/kg	1,589,185 kCal/kg
Efficiency (direct method)	47%	75 % (Designed 70%)
Efficiency (In-direct method)	42%	
Excess air supplied	180%	61.50%
Total heat loss %	58%	25%
Heat loss % due to moisture present	10%	2%
Heat loss % due to dry flue gas	30%	10%
Heat loss % due to H_2O formed by H_2 in fuel	15%	10%
Saw dust consumption	1250 kg	800 kg (40% moisture)
Moisture content of the fuel	40%	40% and dried to 10%

3.6 Verification of the System Using EES Software

Engineering Equation Solver (EES) software is used for the verification of the results of the proposed system. EES can be used to find out the maximization of a given function. Hence it is helpful to determine whether the proposed system is running at its optimum efficiency or not.
Governing equation for the overall efficiency of the plant is

η = 100 – [Dry flue gas + Evaporation of water formed due to H_2 in fuel + Evaporation of moisture in fuel + Other uncountable losses]
Substituting from equation (vii), (viii), (ix) and values for fixed parameters.

$$\eta = 100 - \left[\frac{M1\ X\ 0.23\ X\ (T_f - 27)}{GCV\ of\ fuel}\ \% + \frac{9\ X\ 6.68\{584 + 0.45(T_f - 27)\}}{GCV\ of\ fuel}\ \% + \frac{M3\ X\ \{584 + 0.45\ (T_f - 27)}{GCV\ of\ fuel}\ \% + 3\right]$$

It is assumed here that dried saw dust up to 10% moisture is used for the operation. Research work is suggested a way to dry up the saw dust. GCV of fuel is 3800 kCal/kg and M_3 = 10%.

By using EES graph of efficiency vs O_2 % when stack exhaust temperature is 180 ^{0}C, obtained as shown in Fig. 4.

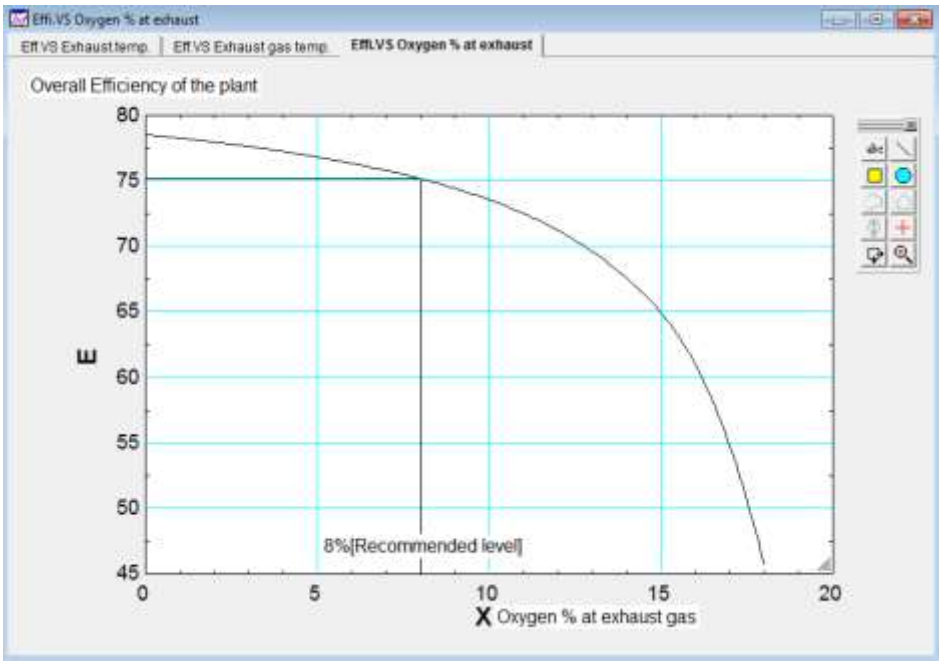

Fig. 4 EES –Overall efficiency of the plant vs oxygen% of exhaust gas

Therefore, it can be concluded that the system is optimized and yielded 75% (Fig. 4) of overall plant efficiency when excess O_2 supply is kept at the range 8%. This can be performed through the adjustment of the ID fan damper. Further, exhaust gas temperature is kept at 180 ^{0}C. This temperature can be regulated when water preheater is operational. Flow rate of the WPH secondary circuit is throttled while monitoring the exhaust gas temperature is settled at 180 ^{0}C. It was assumed here that dried saw dust up to 10%

moisture is used for the operation. WPH secondary circuit and drier design is enclosed in the research to meet the requirement.

4.0 CONCLUSION

Optimizing of thermic fluid heaters are important to reduce fuel consumption through complete combustion. Proper flue gas handling systems help to better use of waste heat for useful work and performance enhancement of the thermic fluid heater.
According to the proposed system, efficiency of the plant can be increased from 42% to 70%, total heat loss can be decreased to 58% to 25% and consumption of the saw dust also can be reduced from 1250kg to 800 kg per month. The analytical results obtained by the indirect method was validated by EE software and the overall efficiency was found as 77%.

REFERENCES

Abeygunawardana, A., (2005) "GLIRICIDIA Fourth Plantation Crop of Sri Lanka," pp. 1–2, 2005

Bierl, C. (2017), Boiler and Pressure Vessel Safety, Hazards in the Workplace American Society of Safety Engineers. USA

Devaraja, U.M.A., Supunsala, S.D.S., Abeysiriwardane, S.W., Gunarathne, R.M.D.S., (2019) Torrefied Biomass Combustion in Biomass Powered Boilers: Process Simulation Based Case Study Analysis of Power Generation and Thermal Energy Generation, National Energy Symposium 2019

Omer A.M. (2008) Ground-source heat pumps systems and applications Renewable and Sustainable Energy Reviews Volume 12, Issue 2, February 2008, Pages 344-371 *https://doi.org/10.1016/j.rser.2006.10.003*

Priyankara Y. and Medagedara T.M (2016) An emerging heating solution for industrial sectors in Sri Lanka. Awareness Programme series on "Safety aspects of boilers and pressure vessels". Federation of Chambers of Commerce and Industry of Sri Lanka (FCCISL).

Rathnasiri, J. (2008) Alternative energy prospects for Sri Lanka. J.Natn.Sci.Foundation Sri Lanka 2008 Vol **36** Special Issue

Sandaruwan. A. (2016). Thermax Sri Lanka representative. *Biomass fired thermic oil heater installations and capacity in Sri Lanka by Thermax*.

Sri Lanka Energy Balance, (2017) An Analysis of Energy Sector Performance. Sri Lanka Sustainable Energy Authority http://www.energy.gov.lk/images/energy-balance/energy-balance-2017.pdf [Accessed: 05- Nov- 2019]

Sri Lanka Sustainable energy authority. (2014). 2014 Energy balance. [pdf]. Available at: http://www.energy.gov.lk/ [Accessed 1st July.2016]

Thermax 2013: Sigma Thermal. (2016). *Thermal fluid heaters*.[Online] Marietta: Available at http://www.sigmathermal.com/thermal-fluid-systems/ [Accessed 15 May.2016]

Wadkinson, M. (2012). *Overview of thermal fluid heaters*. [pdf] New York: NYC 83rd general meeting of the national board. http://www.nationalboard.org/SiteDocuments/General%20Meeting/5-Wadkinson.pdf [Accessed 11 Apr.2016].

Wanson B, (2008). *Practical_Application_Thermal_Fluid_Heating*. [pdf] Hertfordshire. Available at: http:// www.babcock-wanson.co.uk/ [Accessed 11 Apr.2016].

Journal of Engineering and Technology
of The Open University of Sri Lanka (JET-OUSL), Vol. 7, No.2, pp. [44-51], 2019

Effect of different preservatives and temperatures on long term storing for DNA extraction of Ladybird Beetles (Coleoptera: Coccinellidae)

A. G. B. Aruggoda[1*] and Shaukat Ali[2]

[1]Department of Agricultural and Plantation Engineering, The Open University of Sri Lanka, Nawala, Nugeoda, Sri Lanka.

[2]Department of Entomology, College of Natural Resources and Environment, South China Agricultural University, Guangzhou 510642, China.

*Corresponding Author: email: agbar@ou.ac.lk, Tele: +94112881062

Abstract *– High quality DNA for molecular studies can be easily extracted from fresh specimens. However, live samples are difficult to keep for long periods thus making their preservation a serious problem, specially when they are collected and transported from remote locations. In order to establish an efficient method to preserve Ladybird beetles DNA for molecular studies, seven different preservation treatments with different concentrations of ethanol; 95%, 75% at controlled temperatures; – 80^{0}C (Ultra Cold freezing), 4^{0}C and room temperatures (RT) were compared. DNA was extracted from above treatments at three different time periods; 90, 180, 270 days, to analyze the effects of storage durations on quality and quantity of DNA. DNA extracted from fresh specimens was used as control. All treatments were efficient to preserve DNA except insects stored at 75 and 95% ethanol at room temperature, extracted after 270 days, which resulted in gel electrophoresis profile with missing bands. Ultra Cold temperature was the best temperature for the storage even in the presence or absence of ethanol. 95% and 75% ethanol at 4 ^{0}C and room temperature were the second best preservatives for lady bird beetles which had long period of storage up to 180 days with high quantity extracted DNA. In this paper we propose that 95% ethanol is the best chemical preservative for maximizing the quantity and quality of DNA, as well as for maintaining morphological integrity when ultra-cold freezing is not immediately available.*

Keywords*: Insect, Ladybird beetle, DNA extraction, Preservatives, Storage period*

1 INTRODUCTION

Coccinellids (Coleoptera: Coccinellidae) is a highly diversified family of the Coleoptera. Coccinellids are well recognized because of their use as biocontrol agents and this reason has given rise to the subject of many ecological studies throughout the world. As a tropical country Sri Lanka is rich in the species of Coccinellids specially in the areas where crop cultivation take place. Therefore, further studies on their evolution might help on understanding the predatory pattern. However, little is known concerning phylogenetic relationships of the Coccinellidae, and a precise evolutionary framework is still required for the family. At present several researchers interest about studying molecular phylogeny leading to a new era of predatory world.

Molecular phylogeny, which is popular among researchers, provide vast quantities of information for phylogenetic inference and taxonomic identification. DNA sequences provide vast quantities of information for phylogenetic inference and taxonomic identification. It is obvious that obtaining and collecting fresh material is time-consuming, expensive, and often fails to provide a wide coverage of the species (Van Houdt, et al, 2010).

The development of new techniques in molecular genetics carried out by researchers assessing how field collection techniques and preservation practice effects on the condition of the specimens DNA (Post, et al. 1993, Reiss, et al. 1995, Austin and Dillon, 1997; Vogler and Pearson, 1996, Dean and Ballard, 2001, Cor, et al. 2005, Frampton,, et al. 2008). However, several evident limitations exist when using DNA from museum or old specimens; obtaining sufficient amounts of high-quality DNA is a major challenge. Hence, DNA quality use for amplification effected by age, method of storage as well as method of preservation (Van Houdt, et al, 2010). Results of earlier studies indicated that different pretreatment methods can significantly impact the purity and concentration of DNA extracts from dried or old insect specimens (An, et al, 2010; Li, et al, 2015; Pu, et al, 2002; Zang, et al, 2004).

In the present study we researched fresh specimens of Coccinellids stored in ethanol under different temperatures for range of durations for DNA extraction. The objectives of this study were to identify a best-practice approach for storage of high-quality DNA extracts from old specimens, and to test whether ethanol stored specimens can be used successfully for determining reproducible phylogenetic relationships.

3 METHODOLOGY

3.1 Treatments

Seven different preservation treatments, at controlled and room temperatures (RT), were compared: (1) -80 ^{o}C (Ultra cold temperature); (2) 95% ethanol at ultra-cold temperature; (3) 95% ethanol at 4 ^{o}C; (4) 95% ethanol at RT; (5) 75% ethanol at ultra-cold temperature; (6) 75% ethanol at 4 ^{o}C (7) 75% ethanol at RT. DNA extracted from fresh specimens was used as control. In all treatments, specimens were stored for 90, 180 and 270 days prior to DNA extraction. All specimens were kept in darkness for the duration of the experiment. Live *Monechilus sexmaculata* were collected from green houses in South China Agricultural University, Guangzhou and grew in chambers with controlled atmospheric conditions. For all treatments thirty individuals (ten per each storage time) were directly placed in 1.5 ml of preservative for each specimen. For all treatments the ratio of tissue volume to preservative volume was ~1:8.

3.2 DNA Extraction

Abdominal or thorax tissue from each single specimen was used for DNA extraction. An individual beetle was taken from the stock, soaked overnight in 1.5 ml TE buffer (pH 8.0) and dissected to separate the thorax or abdominal tissues. DNA was extracted according to the standard protocol of insect DNA extraction. The selected tissues were crushed in 10 µl STE buffer (10 mM Tris HCl (pH 8.0), 10 mM EDTA (pH 8.0), and 0.15 mM Nacl) added with Protenase K (200 µg/ml), 1:100. The homogenate was digested with another 190 µl of STE and Protenase K buffer at 56 ^{0}C for 3 - 4 hours. In order to digest completely, the mixture was inverted several times during digestion. After digestion homogenate was added with equal volume of Phenol, mixed ten minutes, and centrifuged 12,000 rpm for 4 minutes. Supernatant was transferred to a new 1.5 ml tube and added with Phenol: Chloroform, 1:1, mixed and centrifuged 12,000 rpm, 4 minutes. Chloroform: Isoamyl alcohol, 24:1 added to the transferred supernatant to a new 1.5 ml tube and centrifuged at 12,000 rpm, for 4 minutes. Supernatant was precipitated overnight at -20 ^{0}C added with 1/10 of 3 M NaAc and double amount of total volume of absolute alcohol. Washed the DNA pellet with 70% Ethanol two times, centrifuged at 12,000 rpm, 15 minutes at each time.

Proper dried DNA pellet resuspended in 30 µl TE buffer and preserved at 4 ^{0}C. DNA was quantified at 2:100 dilutions with a Gene Quant II RNA/DNA calculator spectrophotometer (Pharmacia Biotech, Cambridge, UK) at 260 nm wavelength for determination of double-stranded DNA. In order to compare the results, crude DNA was gel electrophoresis and the bands observed were classified into three categories: no band, a very faint band and a very thick band (0, 1 and 2 respectively).

3.3 Experimental design

The statistical analysis of the data on the amount of DNA was made using a completely randomized split-plot design with 10 replications, where the preservation methods were the main plots and storage periods were the subplots. Significance of the electrophoresis results was evaluated using repeated measures within categorical modeling (CATMOD) in SAS (CATMOD; SAS Institute Inc. 1999) at α=0.05. CATMOD bases significance on a chi-squared statistic.

4 RESULTS

4.1 Amount of DNA extracted

The amount of DNA extracted from *Menochilus sexmaculata* by different preservation methods shown in Table 01. There was no significant effect of storage period on the amount of DNA extracted (F=0.14, df=2 and p=0869) but significant differences were observed for preservatives (F=6.28, df=7 and p<0.0001) as well as interaction between storage periods and storage methods. Specimens stored at 75% and 95% ethanol at room temperature consistently had lower yield of DNA in all storage periods, both of these treatments differed significantly from other preservation methods having a detrimental effect upon DNA yield, specially after 290 days (Table 1).

Table 1: DNA yield (ng)/insect extracted from *Menochilus sexmaculata* at 90, 180 and 270 days of storage under various temperatures

Treatments	Storage period (days)			Mean***
	90	180	270	
-80 ^{0}C	116.91	126	107.2	**116.84 ab**
Ethanol 95% at -80 ^{0}C	116.55	151.76	107.14	**125.15 ab**
Ethanol 95% at 4 ^{0}C	99.92	102	98.78	**100.23 bc**
Ethanol 95% at RT †	43.91	44.92	33	**40.61 d**
Ethanol 75% at – 80 ^{0}C	108.75	116.25	26	**83.93 bc**
Ethanol 75% at 4 ^{0}C	61.37	61.02	50.2	**57.53 c**
Ethanol 75% at RT*	29.07	24.22	19.76	**24.35 d**
Fresh specimens	136.70	113.22	253.27	**167.73 a**
Mean	**89.14**	**92.42**	**86.91**	

RT † - Room Temperature

4.2 The effect of temperature on extracted DNA

The effect of temperature on the preservation can also be observed clearly by comparing all the preservation methods. DNA yield extracted under different preservative concentrations, temperature and three different durations are given in table 01. Although the DNA yield was statistically different for all the treatments, the amount of DNA obtained at ultra-cold temperature and 4 ^{0}C was higher than the DNA yield obtained at room temperature (Table 01). Ultra cold temperature was the best for the storage even in the presence or absence of ethanol. The amount of DNA extracted after storage at ultra-cold temperature, 95% ethanol at ultra-cold temperature and 75% ethanol at ultra-cold temperature were 116.84, 125.15 and 83.93 µl respectively.

4.3 The effect of storage period on extracted DNA

Considering the overall mean of three storage periods maximum DNA yield was observed for fresh specimens having a mean value of 167.73 µl of DNA. Apart from this the amount of DNA extracted from treatments, ultra cold temperature and 95% ethanol at ultra-cold temperature was statistically similar having mean values of 116.84 and 125.15 µl of DNA respectively. DNA yields obtained from 95% ethanol at room temperature and 75% ethanol at room temperature were also statistically similar giving 40.16 and 24.35 µl of DNA which was the lowest DNA yield form all treatments.

4.3 The effect of preservation method on extracted DNA

The influence of different preservation methods on DNA quality (considering the quality of bands in gel electrophoresis of crude DNA extracts) are shown in table 02. Highly significant effects of preservation methods ($\chi 2$= 56.5, $p<0.0001$) and interaction between storage period and preservation methods ($\chi 2$=43.97, $p<0.0001$) were observed on DNA quality. All the preservation methods of DNA were almost same quality after 270 days when compared to the control except in the treatments of 95% ethanol at room temperature and 75% ethanol at room temperature. The quality of DNA as the presence or absence of bands in gel electrophoresis as a percentage, isolated from *Menochilus sexmaculata* after storing under different conditions for several periods given in Table 02.

Table 2: Quality of DNA (presence or absence of bands in gel electrophoresis as a percentage) isolated from *Menochilus sexmaculata* after storage under different conditions for several periods

Treatments	Storage period (days)			Mean***
	90	180	270	
-80 ^{0}C	100%(10/10)	100%(10/10)	100%(10/10)	**100%(30/30)**
Ethanol 95% at -80 ^{0}C	80%(8/10)	100%(10/10)	100%(10/10)	**93%(28/30)**
Ethanol 95% at 4 ^{0}C	80%(8/10)	100%(10/10)	100%(10/10)	**93%(28/30)**
Ethanol 95% at RT†	40%(4/10)	30%(3/10)	10%(1/10)	**26%(8/30)**
Ethanol 75% at – 80 ^{0}C	90%(9/10)	90%(9/10)	100%(10/10)	**93%(28/30)**
Ethanol 75% at 4 ^{0}C	60%(6/10)	40%(4/10)	100%(10/10)	**66%(20/30)**
Ethanol 75% at RT†	30%(3/10)	40%(4/10)	20%(2/10)	**30%(9/30)**
Fresh specimens	100%(10/10)	100%(10/10)	100%(10/10)	**100%(30/30)**

Mean	**72%(58/80)**	**75%(60/80)**	**78%(63/80)**

RT† - Room Temperature

As per the Table 2 quality of DNA produced was satisfactory, however; still there was an increase in DNA degradation in all preservation methods after 270 days of preservation. Samples preserved by using ultra cold temperature, 95% ethanol at ultra-cold temperature, 95% ethanol at 4 ^{0}C and 75% ethanol at ultra-cold temperature showed DNA (100, 93, 93 and 93% banding) quality almost similar to the control (100% presence of bands in PCR) whereas samples preserved by using 95% ethanol at room temperature, 75% ethanol at 4 ^{0}C and 75% at room temperature showed degradation in DNA quality when compared to fresh specimens. Specimens stored in 95% and 75% ethanol at room temperature showed unacceptable results for DNA quality producing 26% and 30% of banding at gel electrophoresis of crude DNA. Further, these results demonstrate that extracted DNA of specimens, preserved in 75% and 95% ethanol at room temperature is not suitable for further molecular studies. Table 3 explain the Quality of DNA (appearance of bands in gel electrophoresis as a percentage) isolated from *Menochilus sexmaculata* after storage under different conditions for several periods.

Table 3: Quality of DNA (appearance of bands in gel electrophoresis as a percentage) isolated from *Menochilus sexmaculata* after storage under different conditions for several periods

Treatments	**Storage period (Days)**	**0**	**1**	**2**
-80 ^{0}C	90	0%3(0/10)	90%(9/10)	10%(1/10)
	180	0%(0/10)	50%(5/10)	50%(5/10)
	270	0%(0/10)	100%(10/10)	0%(0/10)
Ethanol 95% at -80 ^{0}C	90	0%(0/10)	50%(5/10)	50%(5/10)
	180	0%(0/10)	20%(2/10)	80%(8/10)
	270	0%(0/10)	50%(5/10)	50%(5/10)
Ethanol 95% at 4 ^{0}C	90	10%(1/10)	80%(8/10)	10%(1/10)
	180	0%(0/10)	100%(10/10)	0%(0/10)
	270	20%(2/10)	70%(7/10)	10%(1/10)
Ethanol 95% at RT†	90	60%(6/10)	40%(4/10)	0%(0/10)
	180	60%(6/10)	40%(4/10)	0%(0/10)
	270	100%(10/10)	0%(0/10)	0%(0/10)
Ethanol 75% at – 80 ^{0}C	90	10%(1/10)	60%(6/10)	30%(3/10)
	180	10%(1/10)	40%(4/10)	50%(5/10)
	270	0%(0/10)	90%(9/10)	10%(1/10)
Ethanol 75% at 4 ^{0}C	90	40%(4/10)	60%(6/10)	0%(0/10)

	180	40%(4/10)	60%(6/10)	0%(0/10)
	270	80%(8/10)	20%(2/10)	0%(0/10)
Ethanol 75% at RT†	90	70%(7/10)	30%(3/10)	0%(0/10)
	180	60%(5/10)	40%(5/10)	0%(0/10)
	270	80%(9/10)	20%(1/10)	0%(0/10)
Fresh specimens	90	0%(0/10)	20%(2/10)	80%(8/10)
	180	0%(0/10)	60%(6/10)	40%(4/10)
	270	0%(0/10)	80%(1/10)	20%(9/10)
Means		26.66% (64/240)	50.00% (120/240)	23.33% (56/240)

RT† - Room Temperature

5. DISCUSSION

There have been several studies on different insect species to try and determine the best taxon-specific preservative for preservation of DNA from specimens collected in the field, and although high-concentration ethanol has been shown to be a generally effective DNA preservation medium (Moreau et al., 2013 and Frampton et al., 2008), there are exceptions to that rule (Fukatsu, 1999 and Vink et al. 2005). Preservation of specimens in 75% and 95% ethanol at room temperature showed a detrimental effect on the amount of DNA extracted after 270 days of preservation. This decrease in the amount of DNA is similar to the findings of other researchers who experienced the same reduction in the quantity of DNA. Post et al. (1993) reported the reduction in DNA recovery with females of *Simulium damnosum* (Diptera: Simullidae) in 80% ethanol at room temperature when compared with 100% ethanol at 4 ^{0}C after 120 days of preservation. Similarly, Reiss et al. (1995) observed a significant decrease in the amount of DNA isolated from Amara glacialis (Mannerheim) (Coleoptera: Carabidae) stored in 95% ethanol at room temperature after only 73 days. Koch et al. (1998) also extracted low amounts of high molecular weight DNA, from the heads of *Simulium vittatum* Zetterstedt preserved in 80% ethanol at room temperature for approximately four years. Cor et al. (2005) found that DNA degradation occurs in tissue stored at room temperature over six weeks in 95% ethanol, and little degradation occurs after five days according to his personal observations.

According to the results of the present study, it is also preferable to store specimens at -80 ^{0}C and 4 ^{0}C. Preserving the quality of both genomic and mitochondrial DNA is of great importance for conducting molecular studies. We found that freezing at –80 ^{0}C was the best method for killing and preserving specimens, but this is often impractical either because specimens cannot be captured alive or because –80 ^{0}C freezing facilities are not available. The use of ultra-cold freezing at has been suggested by Post et al. (1993), Reiss et al. (1995), Dillon et al. (1996), Cor et al. (2005) and Frampton et al. (2008). We also found that preservation in high percentage ethanol is best if specimens are stored at -80 ^{0}C. Post et al. (1993) found that Diptera were best preserved at 4 ^{0}C in 100% ethanol, but they did not tested specimen storage at -80 ^{0}C, Ultra cold freezing which may have produced better results. However, Moreau et al. 2013 found results incorugent to the present study that is 95% ethanol at room temperature as the best preservative for ant species collected in the field. We also recommend that if 95% ethanol is to be used, specimens should be refrigerated or frozen as soon as possible.

The results of our studies have shown that DNA extracted after preservation in 75 and 95% ethanol at room temperature may not be suitable for DNA analysis. These results are similar to the findings of Carvalho et al. (2000). They found that the reproducibility RAPD banding pattern from insect samples preserved in different preservatives at different periods of DNA isolation gave the same banding profile up to 210 days. However different banding pattern was observed with DNA extracted from specimens stored for 360 days in 95% ethanol at room temperature when compared to other preservation methods. The results also suggest that a possible DNA degradation of specimens preserved in alcohol which may be due to the continuing activity of nucleases, which could be inhibited with the addition of EDTA (Dessauer et al. 1990). According to the Frampton et al. (2008) preservative type and concentration affect the quality as well as the quantity of DNA that can be extracted from a given specimen. Additionally, some methods of preservation have adverse effects on morphological characters that need to be preserved for specimen identification.

6. CONCLUSION

Ladybird beetles can be well preserved in preservation methods preferentially in the order of: 95% ethanol at ultra-cold freezing at -80 ^{0}C, in ultra-cold freezing only at – 80 ^{o}C, ethanol at 4 ^{0}C, 75% ethanol at Ultra cold freezing at -80 ^{0}C and 75% ethanol at 4 ^{0}C. Preserving for a period of 9 months at 75 and 95% ethanol at room temperature cannot be accepted due to low DNA levels extracted. We also hope that this will guide biologists in best choice of preservatives for preserving invertebrate tissues for current and future DNA based research.

REFERENCES

An, W.T., Ren, G.D. and Liu, F.S., 2010. Genomic DNA extracting and systematic study of the dry tribe Platyopini specimen of China. J. Hebei Univ., 30, 190–195. (In Chinese)

Austin, A.D. and Dillon, N., 1997. Extraction and PCR of DNA from parasitoid wasps that have been chemically dried. Australian Journal of Entomology, 36: 241- 244.

Carvalho, A. O. R. and Vieira, L. G. E., 2000. Comparison of preservation methods of Atta spp. (Hymenoptera: Formicidae) for RAPD analysis. An. Soc. Entomol. Brasil, 29(3), 489-496.

Cor J. Vink, Steven M. Thomas, Pierre Paquin, Cheryl Y. Hayashi and Marshal Hedin, 2005. The effects of preservatives and temperatures on arachnid DNA. Invertebrate systematics, 19, 99 – 104.

Dean, M. D. and Ballard, J. W. O., 2001. Factors affecting mitochondrial DNA quality from museum preserved Drosophila simulans. Entomologia Experimentalis et Applicata, 98: 279–283.

Dessauer, H.C., Cole, C.J. and Hafner, M.S., 1990. Collection and storage of tissues. p. 25-41. In Hillis, D. M. & C. Moritz (eds). Molecular Systematics, Sinauer, Massachusetts.

Dillon, N., Austin, A. D. and Bartowsky, E., 1996. Comparison of preservation techniques for DNA extraction from hymenop-terous insects. Insect Molecular Biology, 5, 21–24. https ://doi. org/10.1111/j.1365-2583.1996.tb000 36.x

Frampton M. , Droege S., Conrad T., Prager S. and Richards M. H., 2008. Evaluation of Specimen Preservatives for DNA Analyses of Bees. Journal of Hymenoptera Research. Vol.17(2), pp 195-200.

Fukatsu, T. and Shimada, M., 1999. Molecular characterization of Rickettsia sp. in a bruchid beetle Kytorhinus sharpianus (Coleoptera: Bruchidae). Applied Entomology and Zoology, 34 (3), 391–397.

Koch, D.A., Duncan, G.A., Parsons, T.J., Pruess, T.J. and Powers, T.O., 1998. Effects of preservation methods, parasites and gut contents of Black Flies (Diptera; Simuliidae) on polymerase chain reaction products. J. Med. Entomol. 35 : 314-318.

Li, J.L., Zheng, S.Z., Cai, P.; Zhan, G.H. and Gao, Y., 2015. Effects of different pretreatment on DNA extraction from dried specimen of insects. Genom. Appl. Biol., 34, 396–402. (In Chinese)

Moreau, C.S., Wray, B.D., Czekanski-Moir, J.E. and Rubin, B.E.R., 2013. DNA preservation: a test of commonly used preservatives for insects. Invertebrate Systematics 27: 81–86. https://doi.org/10.1071/IS12067

Post, R.J., Flook, P. K. and Millest, A.L., 1993. Methods for the preservation of insects for DNA studies. Biochemical Systematics and Ecology, 21, 85-92.

Pu, M.H., Chen, X.X. and He, J.H., 2002. Extraction of genome DNA from dried specimens of Hymenopteran insects. Zool. Syst., 27, 672–676. (In Chinese)

Riess, R.A., Schwert, D.P. and Ashworth, A.C., 1995. Field preservation of Coleoptera for molecular genetic analysis. Environmental Entomology, 24, 716-719.

SAS Institute Inc., 2004. SAS/STAT® 9.1 User's Guide.Cary, NC: SAS Institute Inc.

Van Houdt, J.K.J., Breman, F.C., Virgilio, M. and De Meyer, M., 2010. Recovering full DNA barcodes from natural history collections of *Tephritid fruitflies* (Tephritidae, Diptera) using mini barcodes. Mol. Ecol. Resour. 10, 459–465.

Vink, C. J., Thomas, S. M., Paquin, P., Hayashi, C. Y. and M. Hedin, C. Y., 2005. The effects of preservatives and temperatures on arachnid DNA. Invertebrate Systematics 19: 99–104.

Vogler, A.P. and Pearson, D.L., 1996. A molecular phylogeny of the tiger beetles (Cicindelidae): congruence of mitochondrial and nuclear rDNA data sets. Mol. Phylogenet. Evol. 6: 321-338.

Zhang, D.H., Zhou, K.Y. and Sun, H.Y., 2004. Comparison of analytical methods for extracting genomic DNA form ethanol-preserved animal specimens. J. Biol., 21, 46–48. (In Chinese)

Journal of Engineering and Technology
of The Open University of Sri Lanka (JET-OUSL), Vol. 7, No.2, pp. [52-58], 2019

Study of the effect of *Aloe vera* gel coating on weight loss of bell pepper (*Capsicum annum* L.) Stored under different temperature levels

R.A.G.D.A. Kumara[1], S.M.A.C.U. Senarathna[2], Thikshani Somarathna[3] and P.K.J. de Mel[4*]

[1, 3, 4] Department of Agricultural and Plantation Engineering, The Open University of Sri Lanka, Nawala, Nugegoda, Sri Lanka.

[2] Food Research Division, Horticultural Research and Development Institute, Peradeniya, Sri Lanka

*Corresponding Author: email: pkmel@ou.ac.lk Tele: +94718673159

Abstract-*Bell pepper (Capsicum annum L.) belonging to family Solanaceae is a popular commercial vegetable growing in Sri Lanka due to its high profit margin. The quick postharvest weight loss is one of the major problems faced by the bell pepper growers in Sri Lanka which causes sevier economic losses. Water loss is the main cause for the postharvest weight loss of bell pepper. Therefore, this study was carried out to investigate the influence of Aloe vera gel coating on postharvest water loss of bell pepper. Healthy 100 bell peppers were randomly selected for the study from a local farmer cultivated under greenhouse conditions. The fruits were rinsed with 25% NaCl solution and air dried. The air dried 100 fruits were randomly divided into 10 sets of 10 bell pepper fruits in each. Four sets were coated with different concentrations of Aloe vera aqueous solutions i.e. 25%, 50%, 75%, 100% respectively and one set without coating was set aside as control and all five sets were stored under ambient temperature (28*℃) . *Other four sets out of five sets were coated with same concentration of Aloe vera aqueous solutions as done in above. The remaining set was kept uncoated as control and all five sets were stored under refrigerator conditions (*4℃). *Coating was performed by hand with the help of clean piece of cloth. All treated fruits under each treatment were air dried for few minutes. Just before storage the fruits were packed separately by using properly punched low-density polypropylene bags and weighed. Each fruit were given an identification number to facilitate data recording. Weight loss in grams of each fruit were recorded once in three days from the commencement of storage (day zero) up to 18 days in bell pepper stored under ambient temperature (28 ^{0}C) and once in seven days up to 49 days in bell pepper stored under refrigerator conditions (4 ^{0}C). The present study revealed that there is a potential for the use of Aloe vera gel coating to minimize postharvest weight loss of bell pepper. It has been proven that the increase of Aloe vera gel concentration used for the coating reduces the weight loss from bell pepper in both storage temperature levels. Pure Aloe vera gel is more effective in reducing weight loss. Further reduction of weight loss can achieve through storing Aloe vera gel coated bell pepper under refrigerator conditions.*

Key words**:** *Aloe vera* wax, *Bell pepper*, water loss

1 INTRODUCTION

Bell pepper (*Capsicum annum* L.) belonging to family Solanaceae is a popular commercial vegetable grow all over the world. The crop originated in central and south America and spread throughout the world in the late 1400s (Bell, 2008).

The edible part of the crop is a three to four lobed fruit having a colour range from green, yellow, orange, purple to red. The fruit can be used in a variety of dishes since its different colors, different taste in ripped and unripe fruits and less pungency. Nutritive value of the food is high since bell pepper can be consumed uncooked or as a salad crop. It is rich in vitamin A, E, C, B6 and Potassium (Arnarson, 2016). Bell peppers are a good source of a mixture of antioxidants including ascorbic acid, carotenoids, flavonoids and polyphenols (Muhammad *et. al.*,2011).

In Sri Lanka this high value crop is cultivated successfully throughout the island specially in protected houses and some open fields. Though the initial cost for the establishment of this crop is relatively high there is a growing interest on cultivation of bell pepper among the farmers due to its high profit margin. The demand for the crop is high both in the local market specially from hotels that cater to tourists and supermarkets as well as the export market.

Though this is a high value crop, it is highly perishable. The quick weight loss of harvested fruits is one of the major problems faced by the growers in Sri Lanka. Water loss is the reason for quick postharvest weight loss which causes severe economic losses to growers. Further water loss causes shrinkage, wilting, softening and subsequent decay of bell pepper. Weight loss also induces senescence and subsequent deterioration. Transpiration and decay are found as the two main causes of deterioration of bell pepper (Kader 1983).

Therefore, it is important to control water loss to minimize postharvest weight loss and ensure postharvest quality of bell pepper. There are techniques to overcome these problems. However, selection of easily available, viable as well as feasible techniques is important (Pandey *et. al.,* 2010).
Coating wax is an age-old practice adopted to protect and ensure extended shelf life of fruits and vegetables (Hardenburg, 1967; Kester and Fennema,1986).

Coating bell pepper using oilseed derived lipid films reduces water loss remarkably (Beaulieu *et. al.*,2009). Chitosan, a biodegradable non-toxic natural substance coating reduced the weight loss and respiration of bell pepper and cucumber and improved appearance (Ahmed *et. al.,* 1991). Application of chitosan inhibits the fungal infections and reduces severity of diseases as well as improve the defense responses in bell pepper (Edirisinghe *et al.,* 2014). Application of edible coatings formulated with arabic, xanthan and pectin gums, candelilla wax and tar bush extract extended the shelf life of bell pepper (Emilio Ochoa Reyes *et. al.,* 2013).

In Sri Lanka too, it is timely to study more and find promising substances to reduced postharvest weight loss of bell pepper, due to the growing interest in bell pepper cultivation and increasing production.

Therefore, this study was carried out to investigate the potential of *Aloe vera* gel as an edible coating to prevent postharvest weight loss of bell pepper.

2 MATERIALS AND METHODOLOGY

2.1 Experimental site

The experiment was conducted in the microbiology laboratory at food research division of Horticultural Research and Development Institute, Gannoruwa, Peradeniya, Sri Lanka.

2.2 Selection of bell pepper

Variety Indra was selected for the trial since it is a productive variety with high quality. The bell peppers were collected from a local farmer who cultivated bell pepper under greenhouse conditions at Pilimathalawa in Kandy District. Randomly selected pest and disease-free healthy bell pepper fruits were hand harvested at the correct maturity. Harvested fruits were properly packed and carefully transported to the laboratory at the food research division.

2.3 Preparation of *Aloe vera* wax

The wax was extracted from the leaves of well matured *Aloe vera* plants grown in a home garden. Harvested leaves were washed thoroughly with 25% NaCl solution to disinfect and the gel matrix was separated (color less hydro parenchyma) from the outer cortex of the leaves. Separated gel matrix was ground thoroughly with the help of a blender and the pulp was filtered using a muslin cloth to remove the fibers and other solid particals. The pulp was pasteurized at 70 ^{0}C for 45 minutes in an electric water bath. Finally, four different aqueous solutions of *Aloe vera* having concentrations of 25%, 50%, 75%, and 100% were prepared by mixing distilled water to the extracted *Aloe vera* pulp. To adjust the pH value of the solutions into 4 citric acid was used. To improve coating efficiency commercial gelling agent Gelatin 1 % was added to the solutions.

2.4 Coating bell pepper

All harvested bell peppers were checked visually for mechanical injuries, disease incidence and any other deformations and altogether 100 equal sized healthy fruits were randomly selected for the trial. Selected fruits were rinsed with 25% NaCl solution to disinfect and air dried. The air dried 100 fruits were randomly divided into 10 sets of 10 bell pepper fruits in each.

Four sets were coated with different concentrations of *Aloe vera* aqueous solution i.e. 25%, 50%, 75%, 100% respectively and one set without coating was set aside as control and all five sets were stored under ambient temperature (28℃) . Other four sets out of five sets were coated with same concentration of *Aloe vera* aqueous solutions as done in above. The remaining set was kept uncoated as control and all five sets were stored under refrigerator conditions (4℃).

Coating was performed by hand with the help of clean piece of cloth ensuring the formation of uniform *Aloe vera* wax film on the entire surface of bell pepper fruits. All treated fruits were air dried for few minutes before storage.

Before storage all 100 fruits were packed separately by using properly punched low-density polypropylene bags. Each fruit was given an identification number with the help of a sticker paste on polypropylene bag to facilitate data recording. Each packed bell pepper fruit was weighed before storage.

2.5 Experimental design and data analysis

Complete Randomized Design (CRD) was adopted in this trial. Data were analyzed by ANOVA using SPSS software. A probability of 0.05% was considered as statistically significant.

2.6 Data Recorded

Weight loss in grams were recorded once in three days from the commencement of storage (day zero) up to 18 days in bell pepper stored under ambient temperature (28 ^{0}C) and once in seven days up to 49 days and once in 14 days from day 49 up to day 77 in the fruits stored under refrigerator conditions (4 ^{0}C).

2.7 Determination of weight loss

Each bell pepper subjected to different treatments was weighed at the beginning of the trial to record the initial weight (IW) and again at the indicated time gaps above during the storage period to record the subsequent weight (SW) of bell peppers. Percentage weight loss (WL) each fruit was calculated by using the following formula.

$$\% \text{ Weight loss (WL)} = \frac{IW - SW}{IW} \times 100$$

3 RESULTS AND DISCUSSION

Water loss is the main cause of postharvest losses in bell pepper. Beauliea *et al.,* (2009) showed that the effective retardation of transfer of water vapor across the skin of bell pepper coated with oilseed derived lipid films from soapstocks. Emilio *et al.,* (2013) revealed the potential of minimizing water loss from bell pepper using edible film coatings formulated with biopolymers (Arabic, Xanthan and Pectin gums), Candedilla wax and tar bush extract. Similar results have been demonstrated by Ahmed *et al*., (1991) by using Chitosan coating for bell pepper in reducing water loss.

The present study too showed us similar results i.e. the retardation of water loss from the bell pepper coated with *Aloe vera* gel. It was obvious that the percentage weight loss was increased with the storage period in all bell peppers coated and uncoated (control) stored under both the temperature levels i.e ambient (28 ^{0}C) and refrigerator (4 ^{0}C) conditions.

However, in both instances i.e ambient temperature (28 ^{0}C) and refrigerator temperature (4 ^{0}C) the percentage weight loss was significantly ($P< 0.05$) less in all treated bell peppers when compared with untreated (control) bell peppers.

3.1 Percentage weight loss of bell peppers coated with *Aloe vera* gel and stored under ambient temperature

The percentage weight loss with the storage period of treated bell peppers stored under ambient temperature are shown in Figure 1. The results showed a significant ($P< 0.05$) variation of weight loss of bell peppers due to different treatments.

The results revealed that the weight loss of bell pepper coated with 100% aqueous solutions of *Aloe vera* gel was less (2.5%) compared to the control where the weight loss was (3%). It is clear with the increment of *Aloe vera* gel concentration i.e. 25%, 50%, 75% and 100% the weight loss is significantly (P< 0.05) reducing from 3% to 2.5% at the 18th day of storage (Figure 1).

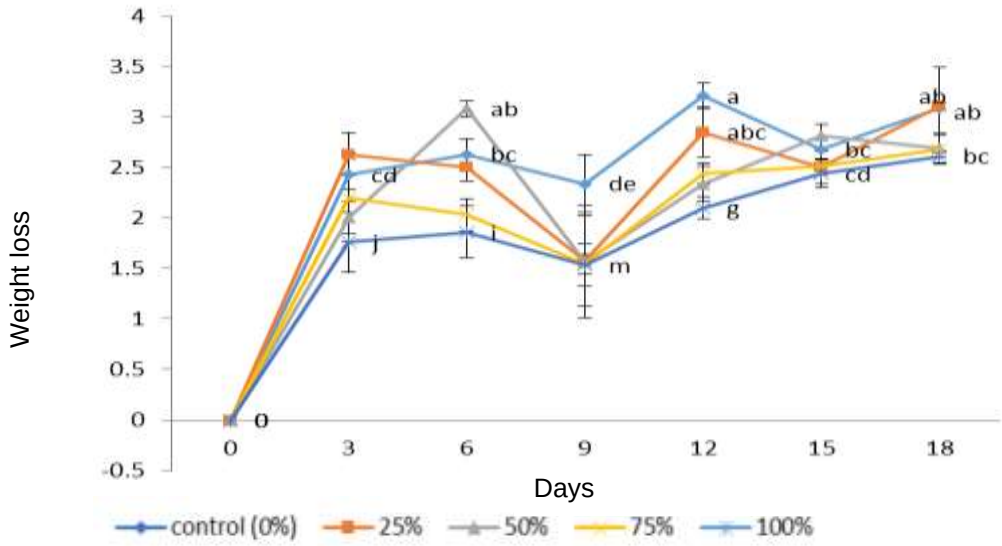

Fig. 1. Change in weight loss (%) of bell pepper treated with different concentrations of *Aloe vera* gel and stored under ambient temperature

3.2 Percentage weight loss of bell peppers coated with *Aloe vera* gel and stored under refrigerator temperature

The results revealed that the weight loss of bell pepper coated with 100% aqueous solutions of *Aloe vera* gel was less (2%) compared to the control where the weight loss was (4%). It is clear that with the increment of *Aloe vera* gel concentration i.e. 25%, 50%, 75% and 100% the weight loss is significantly (P< 0.05) reducing from 4% to 2% at the 49th day of storage (Fig. 2).

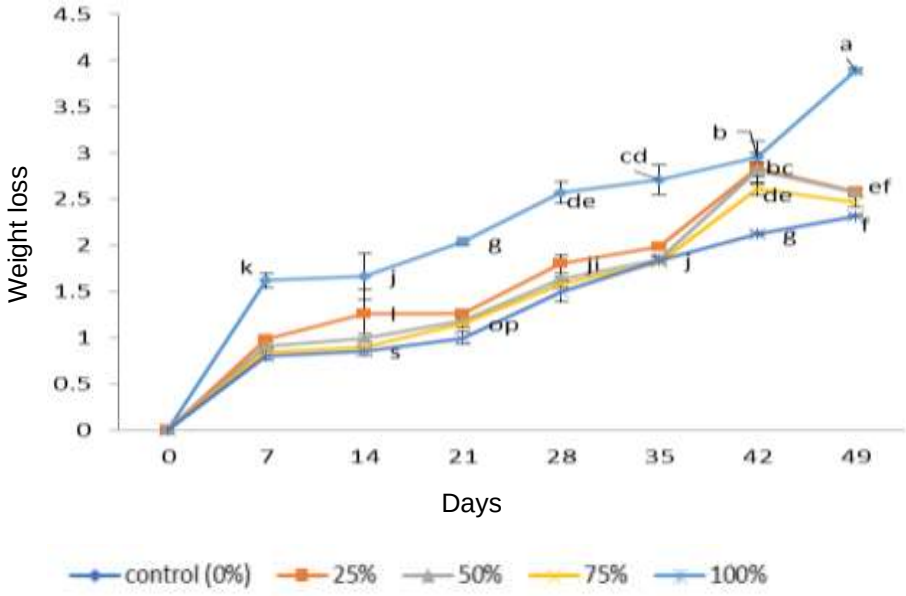

Fig. 2. Change in weight loss (%) of bell pepper treated with different concentrations *of Aloe vera* gel and stored under refrigeration temperature

When comparing the two storage conditions lesser weight loss was observed in bell pepper coated and stored under refrigerator conditions. The weight loss of bell pepper coated with 100% aqueous solutions of *Aloe vera* gel and stored in ambient temperature was 2.5% at the 18th day of storage while the weight loss of bell pepper coated with 100% aqueous solutions of *Aloe vera* gel and stored in refrigerator condition was below 1% at the 21st day of storage. (Fig. 1 and 2).

4 CONCLUSIONS

In conclusion the present study revealed that there is a potential of the use of *Aloe vera* gel coating to minimize postharvest water loss and subsequent weight loss of bell pepper variety Indra. It has been proven that the increase of *Aloe vera* gel concentration used for the coating reduces the water loss from bell pepper. Pure *Aloe vera* gel is more effective in reducing water loss. Further reduction of water loss can be achieved through storing *Aloe vera* gel coated bell pepper under refrigerator conditions.
Further investigations are recommended to study the influence of Aloe *vera* gel coating on postharvest quality parameters of bell pepper

REFERENCES

Ahmed, E.G., Joseph, A., Rathy, P. 1991. Use of Chitosan coating to reduce water loss and maintain quality of cucumber and bell pepper fruits. Journal of food processing and preservation 5(15):359-368 December 1991.

Arnarson, Atli. "Bell Peppers 101: Nutrition Facts and Health Benefits." RSS 20 Authority

Nutrition, July 2015. Web. 7 Feb. 2016.

Beaulieu, J.C., Park, H.S., Ballew Mims, A.G., Kuk, M.S. 2009. Extension of green bell pepper shelf life using oilseed derived lipid films from soapstock. Industrial crops and products 30, 271 – 275.

Edirisinghe, M., Asgar, A., Mehdi, M., Peter, G.A. 2014. Chitosan controls postharvest anthracnose in bell pepper by activating defense-related enzymes. Journal of Food Science and Technology -Mysore- 51(12):4078-4083 · December 2014.

Emilio, O.R., Saul, S., Gabriela, M.V., Julio, C.M. 2013. Improvements of shelf life quality of Green Bell Peppers using edible films coatings formulations. Journal of microbiology, biotechnology and food sciences 2(6):2448-2451 · June 2013

Hardenburg, R.E., 1967. Wax and related Coatings for Horticultural Products. A bibliography.Agricultural Research Service Bulletin, U.S. Department of Agriculture, Washington, D.C

Kader, A.A. 1983. Postharvest quality maintenance of fruits and vegetables in developing countries. In Post-harvest Physiology and and Crop Preservation pp. 455-470 (M.Liberman. ed), Plenum Press, London.

Muhammad Nadeem, Faqir Muhammad Anjum, Moazzam Rafiq Khan, Muhammad Saeed, Asad Riaz. Antioxidant Potential of Bell Pepper (Capsicum annum L.)-A Review. PAK. J. FOOD SCI., 21(1-4), 2011:45-51 ISSN: 2226-5899

Pandey, S.K., Joushwa, J.E. Bisen, a. 2010. Influence of gamma irradiation, growth retardens and coatings on the shelf life of winter guava fruits (*Psidium guajava* L) Journal of Food Science and Technology, 47, 124 – 127.